JOURNAL OF PROTEOMICS 99 (2014) 1–25

Available online at www.sciencedirect.com

ScienceDirect

www.elsevier.com/locate/jprot

Proteolytic events are relevant cellular responses during nervous system regeneration of the starfish *Marthasterias glacialis*

Catarina Ferraz Franco[a], *Romana Santos*[a,b], *Ana Varela Coelho*[a,*]

[a]*Instituto de Tecnologia Química e Biológica, Universidade Nova de Lisboa, Av. da República, 2780-157 Oeiras, Portugal*
[b]*Unidade de Investigação em Ciências Orais e Biomédicas, Faculdade de Medicina Dentária, Universidade de Lisboa, Portugal*

ARTICLE INFO

Article history:
Received 6 September 2013
Accepted 9 December 2013
Available online 14 January 2014

Keywords:
Regeneration
Radial nerve cord
Echinoderm
Proteolysis
DIGE
Starfish

ABSTRACT

The molecular pathways that trigger the amazing intrinsic regenerative ability of echinoderm nervous system are still unknown. In order to approach this subject, a 2D-DIGE proteomic strategy was used, to screen proteome changes during neuronal regeneration *in vivo*, using starfish (Asteroidea, Echinodermata) as a model. A total of 528 proteins showed significant variations during radial nerve cord regeneration in both soluble and membrane protein-enriched fractions. Several functional classes of proteins known to be involved in axon regeneration events in other model organisms, such as chordates, were identified for the first time in the regenerating echinoderm nervous system. Unexpectedly, most of the identified proteins presented a molecular mass either higher or lower than expected. Such results suggest a functional modulation through protein post-translational modifications, such as proteolysis. Among these are proteins involved in cytoskeleton and microtubule regulators, axon guidance molecules and growth cone modulators, protein *de novo* synthesis machinery, RNA binding and transport, transcription factors, kinases, lipid signaling effectors and proteins with neuroprotective functions. In summary, the impact of proteolysis during regeneration events is here shown, although requiring further studies to detail on the mechanisms involving this post-transcriptional event on nervous system regeneration.

Biological significance
The nervous systems of some organisms present a complete inability of neurons to regrow across a lesion site, which is the case of the adult mammalian central nervous system (CNS). Expanding our knowledge on how other animals regenerate their nervous system offers great potential for groundbreaking biomedical applications towards the enhancement of mammalian CNS regeneration. In order to approach this subject, a 2D-DIGE proteomic strategy was used for the first time, to screen the proteome changes during neuronal regeneration *in vivo*, using starfish (Asteroidea, Echinodermata) as a model. We strongly believe in the relevance of our results and have clear evidences that this work constitutes a solid basis for new research on starfish regenerating nerve cord.
We also believe this work will have a significant impact not only on the general scientific community as we present here an alternative animal model to neurobiology, but also on the

Abbreviations: 2D-DIGE, gel difference electrophoresis; CNS, central nervous system; RNC, radial nerve cord; WH, wound healing; RG, tissue re-growth; ECM, extracellular matrix.

* *Corresponding author at:* Instituto de Tecnologia Química e Biológica, Universidade Nova de Lisboa, Av. da República, EAN, 2780-157 Oeiras, Portugal. Tel.: +351 214469451; fax: +351 21441 1277.
E-mail address: varela@itqb.unl.pt (A. Varela Coelho).

1874-3919/$ – see front matter
http://dx.doi.org/10.1016/j.jprot.2013.12.012

scientific community that works with echinoderms or closely related marine invertebrates, which are constantly searching for specific protein markers of several tissues, thus constituting an important advance towards the improvement of large scale protein information of unsequenced, but yet not less important organisms.

1. Introduction

The neurons of some species present a complete inability to regrow across a lesion site, which is the case of the adult mammalian central nervous system (CNS). Several efforts have been made to identify the inhibitory factors present in the environment, which include the neurite outgrowth inhibitory protein *Nogo*, the myelin-associated glycoprotein [1] and the formation of the glial scar, in which reactive astrocytes accumulate in the injury site inducing the modification of the extracellular matrix further disabling the re-growth of neurons (for reviews see [2,3]). In comparison, little is known about the mechanisms that activate the intrinsic growth capacity, and that is why research on organisms that retain the capability to reactivate the intrinsic growth capacity of neurons, such as several invertebrate species including echinoderms, may lead to the discovery of the molecules and pathways behind this trait, a knowledge that might be further applied to the organisms that do not share this ability.

On the basis of their regenerative potential, proximity to Chordates and high genetic homology with humans with over 70% of homologous genes [4], echinoderms are becoming valuable new deuterostome models for the study of regeneration [5–13]. Furthermore, the ability of different echinoderm classes to regenerate their nervous system has been already extensively documented [5,14–18].

Nowadays, there are an increasing number of evidences strengthening the hypothesis that changes in injured axons often occur without the contribution of transcriptional events in the cell body, partly due to the distance between the injury site and the axon nucleus. Additionally to local axonal protein synthesis [19–22], several post-translational events have been implicated in neuronal regeneration such as, proteolysis [22–24], protein phosphorylation [25], ubiquitination [26] and SUMOylation [27,28]. Taken together, these facts clearly highlight that deciphering how the nervous system regenerates has become in part a post-genomic problem, for which proteomic approaches have high adequate answer potential. Despite such compelling evidences, few were the studies that approached regeneration research with proteomic and mass spectrometry tools. King and colleagues [29] used a label-free LC-MS/MS proteomic approach to understand the mechanisms of limb regeneration in larval *Xenopus laevis*. Although a relatively large disagreement in fold changes for the same peptide in replicate measurements, the authors have identified several overexpressed proteins such as matrix metalloproteinases, fibronectin, type I collagen, vimentin, and non-muscle myosin. Interestingly, the authors justify the results' low reproducibility due to the presence of variable post-translational modifications during regeneration. In a more recent study, Saxena and colleagues used a quantitative differential proteomic approach based on 2DE gel analysis and on differential in-gel electrophoresis (DIGE) system, in order to analyze the biomechanisms of zebrafish caudal fin regeneration at several time points after amputation [30]. A total of 41 and 49 proteins were found down- or up-regulated, respectively, during the process of regeneration with the majority of them being responsible for dynamic modulation of actin-based cytoskeleton such as, cofilin, actin-related proteins such as ARP3, and actin and tubulin are themselves up-regulated. Peroxiredoxin 5 was also found up-regulated. This known cellular antioxidant active during inflammation is commonly identified up-regulated during regeneration. Annexin A1 was also found to be regulating the regeneration of zebrafish caudal fin similarly to limb regeneration in *X. laevis* [29].

Proteolytic events have already been reported as having an important role during wound healing and tissue regeneration in other animal models [7,8]. Matrix metalloproteinases (MMPs) [31–33] and calpain proteases [22,23] have important functions in creating a growth permissive environment, by removing neuronal inhibitory constraints, favoring growth cone cytoskeleton fluidity [34] and mediating important signaling events in neuronal regeneration [35–37]. Recently, calpain was also reported to be exclusively phosphorylated in starfish injured radial nerve cords, indicating that this protease might be also orchestrating echinoderm nerve cord regeneration events [5]. Calpain activity has also been reported during intestinal regeneration of sea cucumber *Holothuria glaberrina* [7,8] together with the up-regulation of the ubiquitin–proteasome system [7,8].

The ubiquitin–proteasome system (UPS), known to be responsible for regulating protein degradation in all eukaryotic cells [38], has also been reported as a major player in regulating a multitude of processes and dynamics within the normal neuronal functions, such as gene expression, synaptic and spine functions, and neuronal degeneration by tagging for elimination of key proteins required for morphological and chemical neuroplasticity (for reviews on the UPS functions within nervous systems see [39–42]). The UPS also plays a main role during neural development [26]. In fact, Verma et al. [43], showed that an impaired UPS function resulted in poor regeneration of isolated growth cones in cultured rat sensory axons, which is in accordance with reports of an increase in ubiquitin mRNA after axotomy [44], suggesting an enhanced requirement for ubiquitin during axonal regeneration.

Nowadays it is increasingly being accepted that proteolysis is necessary for the success of regeneration. However, only few mechanisms have been proposed to explain how proteolysis mediates regeneration events [24].

In this study we present a proteomic characterization of the neuronal regeneration events of the starfish *Marthasterias glacialis* after arm tip amputation. The difference gel electrophoresis approach (DIGE) was used to compare the RNC proteomes from injured starfish and their respective uninjured controls collected at 48 h, 13 days and 10 weeks post-arm tip

ablation (PAA). A dramatic proteome modulation by proteolysis was observed during RNC wound healing events. Modulation of protein amounts via proteolysis was also detected during RNC functional re-growth. Such results suggest that localized protein amount modulation is also important for the onset of regenerative events, sustaining the hypothesis that proteolysis has an important role in both inducing and maintaining the regenerative machinery throughout functional neuronal tissue re-growth.

2. Materials and methods

2.1. Experimental groups and regeneration induction

Thirty six adult specimens of the starfish *M. glacialis* (Linné, 1758) were collected and regeneration was induced as previously described [5]. Briefly, starfish with no previous signs of regeneration were collected and divided in 6 groups, 3 control groups and 3 regenerating groups, each composed of 6 animals. After anesthetizing starfish with 4% (w/v) magnesium chloride in 50% (v/v) artificial seawater, regeneration was induced by amputation of the arm tip at 2/3 of the way down to the arm, with 2 arm tips amputated per animal. The control and regenerating groups were kept throughout the course of the experiments in the same conditions (open-circuit tanks with re-circulating sea water at 15 °C and 33‰) at Vasco da Gama Aquarium (Oeiras, Portugal).

2.2. Collection of radial nerve cords during wound healing (WH) and re-growth (RG) of the arm tip

The RNC, located at the oral plane of the starfish body and separated from the external environment by a thin epithelia, was extracted from the radial canal with a pair of tweezers as previously described [5]. RNC wound healing events (WH) were studied at two-times, 48 h and 13 days post-arm tip ablation. Altogether, 12 regenerating and 12 non-regenerating starfish were used for the experiments, from which two RNCs were collected per starfish. This was achieved by extracting only the first centimeter from the arm tip upwards, in order to restrict our analysis to tissue adjacent to the injury plane. The collected tissues were immediately immersed in an ice-cold solution of phosphate buffered saline (PBS) supplemented with protease, kinase and phosphatase inhibitors (Complete antiprotease kit from Sigma; 4 μM cantharidin; 4 μM staurosporine and 1 mM sodium orthovanadate), flash frozen in liquid N_2 and conserved at −80 °C until further use.

Ten weeks after injury, the newly regenerated arm tip was approximately 7–10 mm in length. The regenerated RNCs were carefully excised and processed as explained above. Again, two regenerated RNCs were extracted per starfish, and a total of 6 regenerating and 6 non-regenerating starfish were used in the experiments.

2.3. Radial nerve cord soluble and membrane protein-enriched fractions

For protein extraction, the collected control and injured RNCs were disrupted using the automated frozen disruption procedure as previously described [45]. Briefly, the deep frozen RNC (in liquid N_2) was placed in a previously chilled teflon sample chamber containing four stainless steel beads (5 mm diameter). The chamber was placed in a Mikro-Dismembrator (Sartorius) and set to 3000 rpm for 60 s. To avoid sample loss, the resulting powder (still in a deep frozen state) was resuspended with vigorous agitation inside the teflon chamber for 3 min, in hypotonic lysis buffer (2×) supplemented with protease, kinase and phosphatase inhibitors (20 mM HEPES, pH 7.4; complete protease inhibitor cocktail; 4 μM cantharidin; 4 μM staurosporine and 1 mM sodium orthovanadate). After removal of cellular debris and insoluble material (100 ×*g*; 10 min; 4 °C), the total cellular membranes were collected from the homogenate by ultracentrifugation at 55,000 rpm, 3 h, 4 °C using an Optima-Max E Ultracentrifuge with the TLS-55 rotor (Beckman-Coulter). The membrane pellets were gently washed in ice-cold 1× PBS also supplemented with protease, kinase and phosphatase inhibitors (complete protease inhibitor cocktail; cantharidin 2 μM; staurosporine 2 μM and sodium orthovanadate 0.5 mM, Sigma). In order to collect the washed membranes, another ultracentrifugation step was performed. Supernatants containing the total soluble proteins were precipitated with trichloroacetic acid (TCA) 10% (w/v), β-mercaptoethanol 0.07% (v/v) and the protein pellet washed with ice-cold acetone with 0.7% (v/v) β-mercaptoethanol for complete removal of the TCA. Both membrane (M) and soluble (S) protein-enriched fractions were frozen at −80 °C until further analysis.

2.4. Difference gel electrophoresis (DIGE)

2.4.1. Protein labeling

The prepared enriched protein fractions were resuspended in DIGE labeling buffer [7 M urea, 2 M thiourea, 1 M Tris buffer, 4% (w/v) CHAPS, Complete antiprotease kit (Sigma), pH 8.5] and gently shaken (4 °C) to achieve complete solubilization of protein extracts. The pH was carefully re-adjusted to 8.5 using NaOH solutions (1–100 mM). The total protein concentration was determined using the 2D Quant Kit™ (GE Healthcare). Both protein-enriched fractions were then labeled with Cyanine 3 or 5 (Cy3, Cy5) fluorescent dyes (GE Healthcare) according to the manufacturer instructions (400 pmol CyDye to 50 μg of total protein). To ensure that all labeling reactions took place simultaneously, CyDyes were added to the tube caps, and then put in contact with the samples by a simultaneous quick spin down of all the reaction tubes. Labeling reaction was performed for 25 min on ice and in the dark. After this, 10 nmol of lysine (1 μl of a 10 mM solution) was added to each reaction tube cap and, after 5 min, the labeling reactions were simultaneously quenched by a quick spin down of the tubes, which were then kept on ice for another 10 min. The same procedure was applied to the internal standard, a pool of all samples (control and regenerating groups), which was then labeled with Cy2 fluorescent dye (GE Healthcare). The internal standard was used on all gels to ease image matching and cross-gel statistical analysis. Prior to sample multiplexing, equal volumes of sample buffer (8 M urea; 130 mM DTE; 4% (w/v) CHAPS and 1% (v/v) of the correspondent pH range ampholytes) were added to each of the labeled protein samples. Then, rehydration buffer (8 M urea; 13 mM DTE; 4% (w/v) CHAPS and 0.5% (v/v) of the correspondent

pH range ampholytes) was added up to a final volume of 450 μl prior to isoelectric focusing (IEF). Each strip was actively rehydrated overnight at low voltage (30 V) with 120 μg of multiplexed RNC soluble protein extracts or with 150 μg of RNC membrane protein extracts. The 6 biological replicates per group were multiplexed randomly and the fluorescent dye was swapped within the groups in order to prevent preferential labeling and bias results in-gel image analysis.

2.4.2. Protein separation and image acquisition

For protein separation according to their *pI*, 3–10 pH range 24 cm IEF strips were used (see Supporting information 1 for IEF protocols). Prior to SDS-PAGE, the strips were equilibrated in a two-step process with a buffer (50 mM Tris–HCl pH 8.8, 6 M urea, 30% (v/v) glycerol, 2% (w/v) SDS, 0.002% (w/v) bromophenol blue) containing first 2% (w/v) DTE and then 4% (w/v) iodoacetamide. Protein separation in the second dimension was performed in 24 cm SDS-PAGE gels (12.5% (w/v) acrylamide). Electrophoresis was carried out at 38 mA/gel in the running buffer (25 mM Tris, pH 8.8; 192 mM glycine, and 0.2% (w/v) SDS) until the bromophenol blue reached the bottom of the gel.

All gels were scanned using the Fujifilm FLA-5100 Fluorescent Image Analyzer (GE Healthcare). The Cy3 images were scanned using a 532 nm laser and a 580 nm band pass (BP) emission filter; Cy5 images were scanned using a 633 nm laser and a 670 nm BP emission filter and; the internal standard (Cy2) gels were scanned using the 457 nm laser and the 610 nm BP emission filter. All gels were scanned at 100 μm pixel size.

2.4.3. Gel image and statistical analysis

All gel images were exported into Progenesis SameSpots, v. 3.1 (Nonlinear Dynamics), where quantitative and statistical analyses of protein spots were performed. For protein quantification, gel spot volumes (an integration of optical density and area) were measured as a percentage of the total volume of all detected spots and then log transformed to obtain a normalized distribution. Three types of statistical analysis were performed using the normalized spot volumes for each WH an RG condition: 1) a Power Analysis to evaluate if the number of biological replicates used were sufficient to account for the inter-individual variability, 2) a Principal Component Analysis (PCA) to verify the relative distribution of all biological replicates of each experimental group (WH at 48 h, 13 days and RG at 10 weeks post-arm tip ablation and the corresponding controls); and 3) an analysis of variance (ANOVA) for all spots in the PCA groups in order to detect significant variations by setting the threshold to a p-value <0.05.

2.4.4. Preparative gels, spot picking, in-gel digestion and MALDI-TOF/TOF analysis

High protein load 24 cm 2DE preparative gels were run in duplicate for the WH and RG DIGE experiments. Each 2DE gel contained either 600 μg of the total protein with a pool of all control samples or, 400 μg total protein with a pool of all regenerating samples (Supporting information 1). The 2DE gels were fixed and then post-stained with colloidal Coomassie (CCB) [46]. The CCB stained gels were scanned using the Fujifilm FLA-5100 Fluorescent Image Analyzer (GE Healthcare) using the red laser without an emission filter. The subsequent gel image was exported into Progenesis SameSpots and matched with the DIGE gel images. Spots of interest were selected and manually excised from the preparative gels either in pools of matched spots, if the spot of interest was of low abundance, or individually, if it was an intensely stained spot. Excised spots were *in-gel* digested, as described elsewhere [47] (Supporting information 1) and tandem mass spectrometry was performed using a MALDI-TOF/TOF 4800 plus mass spectrometer (Applied Biosystems).

2.4.5. Protein identification, BLASTp searches and gene ontology annotation

Protein identification was performed using two different search algorithms, MOWSE (MASCOT, version 2.2; Matrix Science, Boston, MA) and Paragon (ProteinPilot, version 3.0, revision 114732; Applied Biosystems, USA) and three protein sequence databases (Supporting information 1).

In order to integrate and compare the protein identification results generated by the two search algorithms and three protein sequence databases, the software tool COMPID was used [48]. Two types of reports were then generated for each cellular fraction, S and M, containing the information of all the peptides and proteins common and unique to each search algorithm. Protein identifications were considered common between different algorithms if having at least one peptide with a strictly equal amino acid sequence, with the exception of the isobaric amino acids I and L, and Q and K. Since this tool was designed to compare protein identification data derived from LC-MS/MS experiments, only MS/MS data were used for the comparison.

Similarly as previously described [5,47,49], most of the identified proteins were homologous to *Strongylocentrotus purpuratus* proteins. Since the sparse information on Gene Ontology categories (GO) of *S. purpuratus* proteins impaired the success of data interpretation, a protein–protein BLAST (BLASTp) search was performed through BLAST2GO java application (http://www.blast2go.de). This enabled the performance of GO annotation of the identified proteins in the starfish RNC by using GO categories of the best hit derived from the BLASTp results (BLASTp minimal Expectation value set to $<1 \times 10^{-3}$).

3. Results

The morphological events of starfish arm regeneration have been extensively studied and characterized in several asteroid species such as *Asterias rubens* [50,51], *Leptasterias hexactis* [52] and *Asterias rollestoni* [53]. In starfish, the morphallactic process of regeneration seems to be the main motor of tissue replacement and re-growth due to the absence of a blastema-like structure formation as the center of cell proliferation. According to these evidences the proposed working hypothesis for the morphallactic process of arm regeneration in starfish includes four phases: (1) wound healing with the accumulation of immune cells at the wound site (1st week PAA), (2) migration of distant non-aging cells of mixed origin, including the pyloric caeca and coelomic epithelium (12–14 days PAA), (3) proliferation in these organs to compensate for cell loss, and

finally (4) local proliferation in the regenerating arm (up to 10–15 weeks PAA) [51,54]. In order to study the RNC injury response and tissue re-growth, regeneration was induced by amputating starfish arm tips (Fig. 1A and B). To study wound healing events (WH), RNCs were collected at 48 h and 13 days post-arm tip ablation (PAA) and, to study the re-growth phase (RG), RNCs were collected 10 weeks PAA. Soon after 10–15 h PAA, a contraction of the tissues surrounding the injury plane was observed, stopping the leakage of body fluids. At 48 h PAA, the connective tissue began to accumulate at the wound edges, bridging the gap created by arm tip amputation (Fig. 1C). At approximately two weeks after injury (13 days), the wound is completely sealed, however it is still not possible to observe traces of a re-growing arm (Fig. 1D).

At ten weeks PAA, it is possible to observe a regenerated arm tip with a length of approximately 7–10 mm (Fig. 1E). The RNC also has regenerated, showing only a difference in thickness when compared with the same tissue in the zone preceding the injury plane.

To increase the number of proteins to be detected in 2DE the collected nerve tissues from both regenerating and non-regenerating starfish were pre-fractionated into soluble and membrane protein-enriched fractions.

Several statistical analyses were performed on the obtained DIGE results within Progenesis SameSpots. A power analysis revealed that the number of biological replicates used in the experiments (6 animals per group) was adequate to account for the inter-individual variability. In addition, the Principal Component Analysis of individual DIGE gels showed a clear separation of each experimental group and the respective controls (Supplementary Fig. 1). However, the gels from the samples collected at 48 h and 13 days PAA showed close correlation and clustered together, for both soluble and membrane enriched fractions. For this reason, the analysis of variance was performed between controls and only two injured groups, wound healing (WH) (including 48 h and 13 days PAA and the respective controls), and re-growing RNC (RG) (10 weeks PAA and the respective controls). This analysis detected a total of 197 and 90 spots with significant volume variation ($p < 0.05$ and fold >1.5), respectively, in the soluble and membrane fractions of WH RNC DIGE gels in comparison with controls, of which 185 and 85 spots from the WH soluble and membrane fractions, respectively, were manually excised. For RG RNC DIGE gels, 149 and 53 spots from the soluble and membrane fractions, respectively, had a significant change ($p < 0.05$ and fold >1.5) in the relative spot volumes when compared with the respective controls. From the correspondent RG preparative gels, 149 and 52 spots were excised for protein identification, from the soluble and membrane fractions.

After in-gel digestion of the excised spots and analysis by MALDI-TOF/TOF, the obtained spectra were processed with two protein identification search algorithms and three protein sequence databases in order to achieve both complementary and confirmatory protein identification results (Supplementary Tables 1 and 3) as previously reported [47,49]. Among the excised spots from the soluble and membrane fractions of the WH group, 281 different proteins were inferred (207 and 74 different proteins in the soluble and membrane fractions, respectively) (Supplementary Table 2). For the RG group, a total of 247 different proteins were inferred (184 and 63 different proteins in the soluble and membrane fractions, respectively) (Supplementary Table 4).

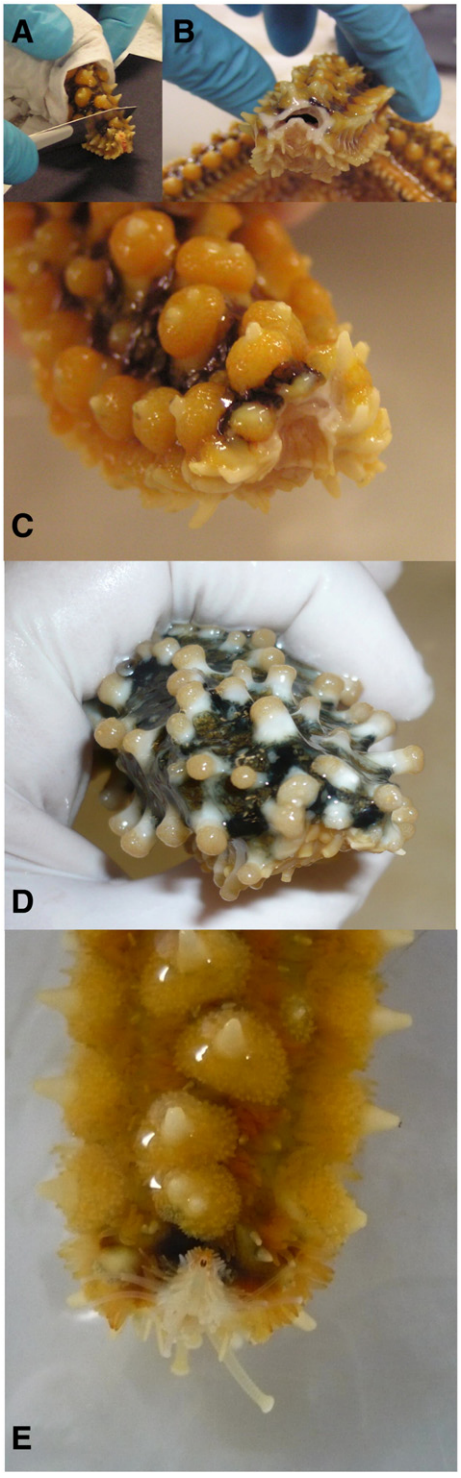

Fig. 1 – Several stages of *Marthasterias glacialis* arm regeneration events. (A) Induction of regeneration by arm tip ablation. (B) Wound immediately after amputation. Wound healing (WH) time points: 48 h (C) and 13 days (D) post-arm tip ablation. (E) Tissue re-growth (RG) time point after 10 weeks post-arm tip ablation.

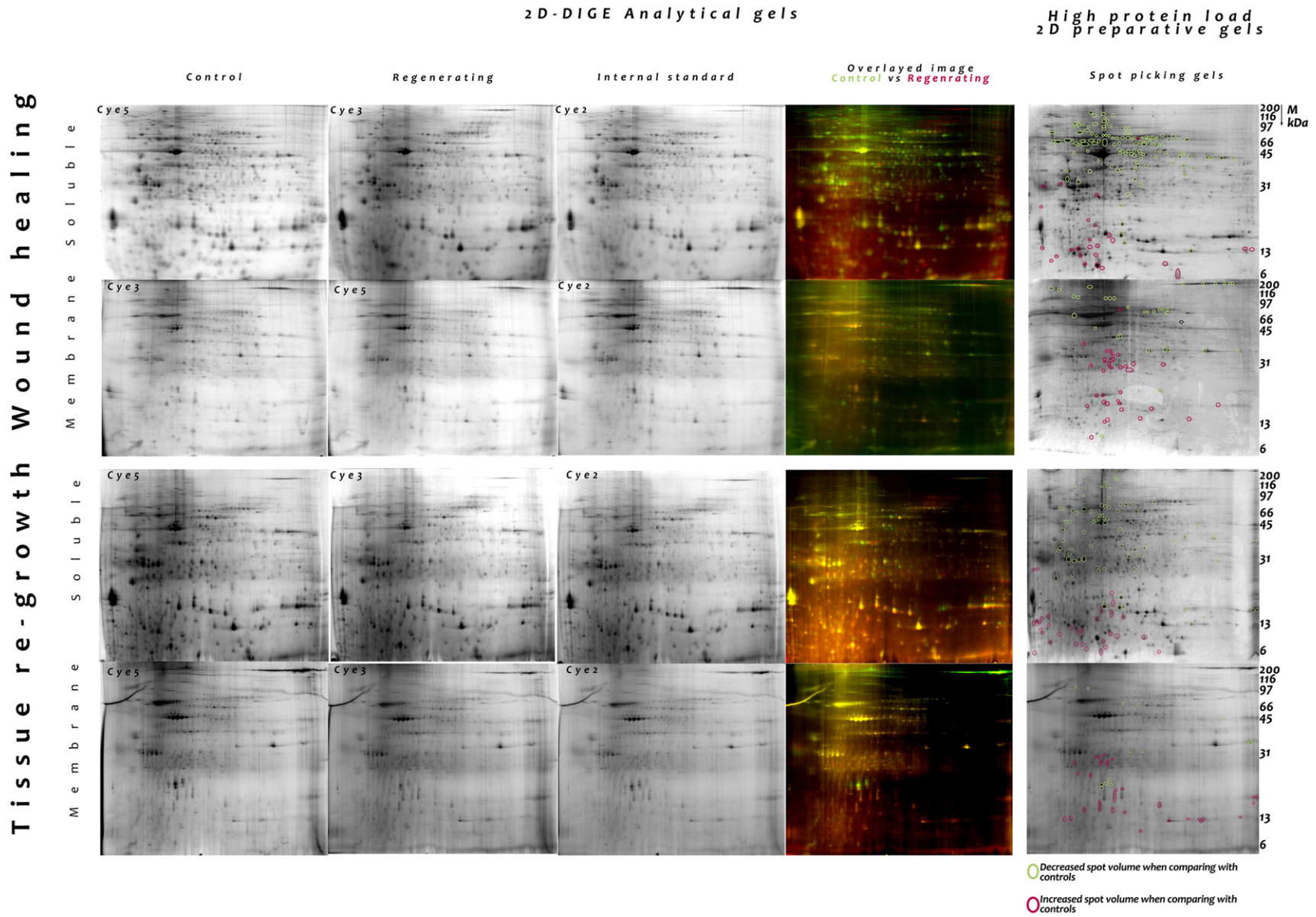

Fig. 2 – DIGE gels for the control and regenerating groups and for the internal standard are presented on the three first left columns. In the DIGE overlayed images of the controls vs regenerating radial nerve cords, for each regenerating time point, it is possible to see that in the high mass region of the gel the spots show higher volumes in the control group (green spots) and, in the low mass region of the gel higher volumes are shown for the regenerating group (red spots). On the preparative gels on the right column, spots that were picked for protein ID are labeled with green (up-regulated proteins in controls) and red circles (up-regulated proteins in regenerating RNC).

From both nerve subcellular fractions of the two assayed regeneration stages, a considerable amount of inferred proteins derived from a single peptide identification ($p < 0.05$) (Supplementary Tables 1 and 3; Supplementary Fig. 2), most probably due to the lack of starfish protein sequences on the available public databases. Another possible hypothesis for the identification of few peptides per protein could be related with the existence of post-translation modifications. In fact, several of the identified proteins had an apparent molecular mass (M) above the predicted by its sequence (Supplementary Tables 2 and 4), concomitantly with a shift in the *pI* apparent values. This effect has already been described in several 2DE studies aiming to understand protein dynamics in regenerating neurons [35,55].

In the DIGE overlayed images of the WH and RG RNC with their respective controls from both soluble and membrane fractions (Fig. 2) it is possible to observe that the high molecular mass (M) region of the control gels shows a considerable amount of spots with significant superior spot volumes. In opposition, the low M protein spots are generally more abundant in the regenerating RNC DIGE gels. This 2DE pattern is characteristic of proteolytic events occurring during the biological process.

To understand how proteins and pathways are being modulated through proteolysis in the RNC WH and RG events, the predicted M (*Mpred*) of the identified proteins were compared with the apparent M (*Mappar*) determined based on the spot positions in the 2DE gels (Supplementary Tables 1 and 3). For protein spots localized in the 2DE mass region (M) of 116–200 kDa, proteins were considered as having no mass change if the observed shift was inferior to 40 kDa; if the spots were localized in the 45–116 kDa region, the established margin was of 13 kDa; for the M region of 31–45 kDa, 5 kDa margin was permitted and finally, for the 6–31 kDa M region, a 4 kDa shift was allowed (Supplementary Table 5). According to this evaluation, the identified proteins in the regenerating (WH and RG) groups were divided in three categories:

1) Proteins with decreased M: if the Mappar < Mpred,
2) Proteins with no M change: if the Mappar ≈ Mpred;
3) Proteins with increased M: if the Mappar > Mpred.

Identified proteins were further categorized as being fragments; proteolysis substrates/down-regulated and up-regulated by adding to the above-described categories for mass shift, the respective variation of the relative spot volumes between the

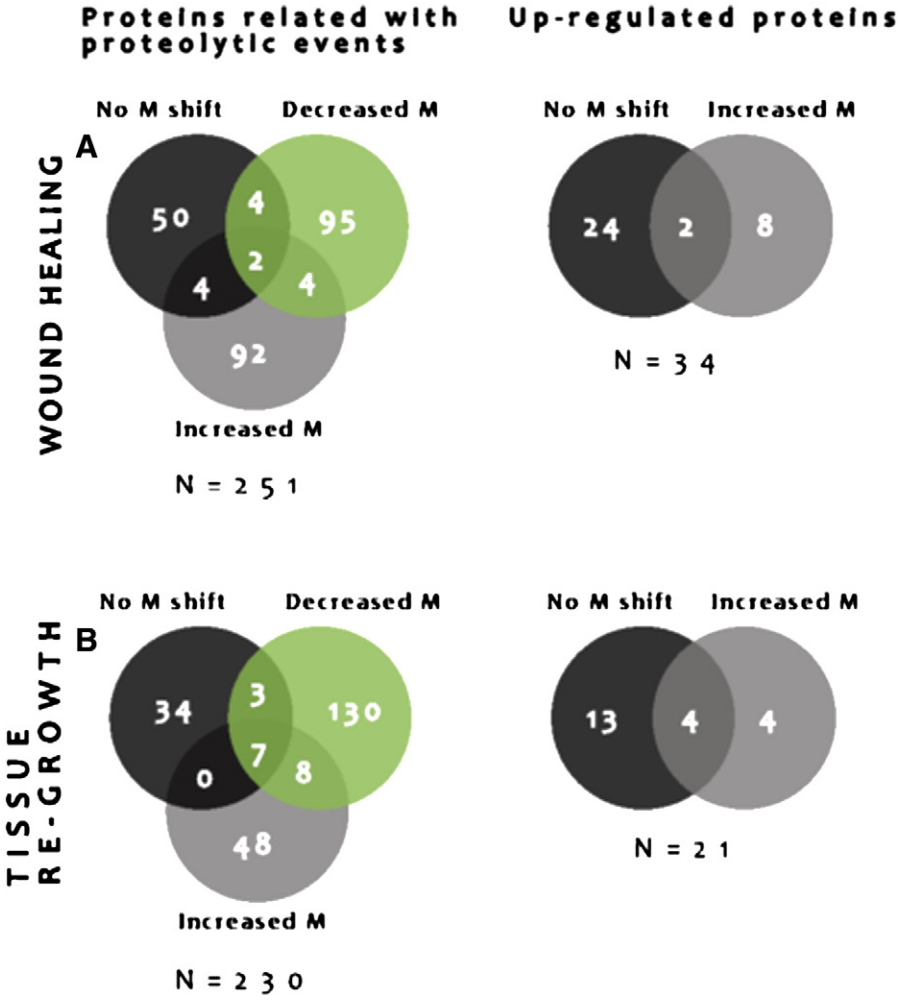

Fig. 3 – Number of identified proteins categorized in terms of molecular mass shifts in both soluble and membrane fractions during radial nerve cord wound healing (A) and re-growth (B) events.

Table 1 – List of some of the identified proteins associated with *Marthasterias glacialis* radial nerve cord wound healing (48 and 13 days PAA) and re-growth (10 weeks PAA) events in both soluble and membrane enriched fractions. *Hypothetical/uncharacterized proteins that had a significant hit on the *BLASTp* searches. The name of the *BLASTp* search best hit is here presented. The complete lists of identified proteins are available in Supplementary Tables 2 and 4 for WH and RG, respectively, with the correspondent information on the performed *BLASTp* searches.

Protein name	Accession number	General function	RNC fraction	Regeneration stage	Spot(s)	Predicted mass (kDa)	Apparent mass on the 2DE (kDa)	Mass shift	Injury relation category			Number of fragmented peptides
									Up-regulated	Proteolysis substrate or down-regulated	Fragment	
30S ribosomal protein S21	Q04T16	RNA interaction or translation regulator	S	WH	530	8	97	↑		●		1
30S ribosomal protein S8	sp|B2GDV5	RNA interaction or translation regulator	S	RG	4122	15	17	=		●		1
40S ribosomal protein S21	Q6AZJ9	RNA interaction or translation regulator	M	WH	3804	9	8	=	●			1
40S ribosomal protein S21	sp|Q6AZJ9	RNA interaction or translation regulator	S	RG	5370	9	9	=	●			1
50S ribosomal protein	sp|A0R8J2	RNA interaction or translation regulator	S	RG	848; 982; 1786; 2211; 4570; 4712; 5335; 5573; 5590; 6142	20	8–13; 45–119	↓/↑		●	●	1
54S ribosomal protein L4, mitochondrial	sp|A5DH98	RNA interaction or translation regulator	S	RG	6076	35	17	↓		●		1
Actin	P07828	Cytoskeleton dynamics	S	WH	65; 149; 155; 430; 511; 523; 622; 964; 1282; 1290; 1622; 1623; 1631; 1637; 1640; 1653; 1660; 1661; 1668; 1690; 1697; 3951; 4092; 4109; 4149; 4169; 4338; 4444; 4574	31–42	9–14; 50–284	↑/=/↓		●	●	>15
Actin	B0FBP2	Cytoskeleton dynamics	M	WH	1792; 2200; 2329; 2486; 2520; 2554; 2646; 2692; 2837; 2848; 2894; 3197; 3449; 3583; 3662; 3665; 4012	31–42	9–13; 20–55	=/↓	●	●	●	>15
Actin	sp|P07828	Cytoskeleton dynamics	M	RG	1311; 2004; 2085; 2118; 2203; 2223; 2224; 2307; 2345; 2357; 2417; 2433; 2593; 2620; 2630; 2732; 2738; 2748; 2750; 2796; 2966; 3047; 3125; 3130; 3140; 3142; 3157; 3163; 3174; 3737; 3747; 3748; 3766; 3768	42	13–64	↑/↓		●	●	>12
Actin	gi|115918029	Cytoskeleton dynamics	S	RG	952; 1656; 2047; 4306; 5167; 1865; 5100; 1655; 920	42	10–15; 56–97	↑/↓		●	●	>8

Actin CyIIb Cytoskeletal	gi|115918029	Cytoskeleton dynamics	M	RG	2657; 2681; 3079; 3147	42	13-22	↓		●			>12
Actin-related protein 2/3 complex subunit 5	C3Z4W4	Cytoskeleton dynamics	M	WH	3172	17	20	=	●				1
Allograft inflammatory factor	Q0H8V2	Calcium related/ cytoskeleton dynamics	S	RG	4047	17	17	=	●				1
Alpha-actinin-1	sp|Q2PFV7	Cytoskeleton dynamics	S	RG	4802	103	12	↓				●	1
Ankyrin	B2KC90	Growth cone and axon guidance/cytoskeleton dynamics	S	RG	1657	39	70	↑		●			1
ATP-binding cassette sub-family A member 7	sp|Q7TNJ2	Transport/cytoskeleton dynamics/lipid metabolism and transport	S	RG	4673	238	13	↓		●			1
Axonemal 84 kDa protein	Q8T880	Transport	S	WH	2752	84	31	↓		●			1
Beta-G spectrin (CRE-UNC-70 protein)	UniRef100_ E3LPH0	Calpain activity evidences/growth cone and axon guidance/ developmental/ cytoskeleton dynamics	S	RG	6033; 6149	272	33–41	↓		●			2
BH2562 protein	Q9K9T3	Hypothetical/unkown	S	WH	4338; 4894	27	11, 48	↑/↓		●		●	2
Calmodulin	P69097	Kinase or kinase regulators/calcium related	S	WH	4207; 4269; 4373	17	10, 11, 12	↓				●	3
Calmodulin	Q32VZ5	Kinase or kinase regulators/calcium related/ apoptosis/developmental/ cytoskeleton dynamics	S	RG	3177; 4431; 4481; 4495; 4516; 4570; 4576; 4662; 4802; 4840; 4953; 4966	15–17	11–30	↑/=/↓	●			●	>3
Calreticulin	Q8IS63	Calcium related	S	WH	842	47	87	↑		●			9
Cat eye syndrome critical region protein 2	115918080	Transport/apoptosis	S	WH	1690; 1713	202	54	↓		●			2
Cdc42 small GTPase	D0EVY0	Kinase or kinase regulators/ growth cone and axon guidance/cytoskeleton dynamics	M	WH	3022	21	25	=	●				2
cGMP-dependent protein kinase, isozyme	E0W2T9	Kinase or kinase regulators	M	RG	2681; 2732	121	20–21	↓		●			2
Chaperone protein htpG	sp|P0A6Z3	Folding/Neuroprotection	S	RG	976	71	94	↑		●			10
Chaperonin containing TCP1, subunit 5 (epsilon)	P80316	Transport/Folding	S	WH	1157	60	75	↑		●			3
Cysteinyl-tRNA synthetase	Q0BKI3	RNA interaction or translation regulator	S	WH	2735	53	31	↓				●	1
Cytochrome P450 19A1 (Fragments)	sp|P79699	Neuroprotection	S	RG	1792	37	66	↑		●			1
Cytosol aminopeptidase	sp|Q2IX74	Endopeptidases or proteases	M	RG	3749	52	38	↓		●			1
Dihydropteridine reductase (Fragment)	UniRef100_ D5LPS8	Neuroprotection	M	RG	2203	16	31	↑	●				1
dihydropyrimidinase, partial	115969215	Developmental	S	WH	1110; 1120; 1123; 1384	71–76	66–67	=/↓		●			4
Dihydropyrimidinase, partial	Q5DF26	Developmental	M	WH	1003; 1050; 1056	62	77	↑		●			5
Dyp-type peroxidase family protein	UniRef100_ D2B1J7	Neuroprotection	M	RG	2966	49	16	↓				●	1

(continued on next page)

Table 1 (*continued*)

Protein name	Accession number	General function	RNC fraction	Regeneration stage	Spot(s)	Predicted mass (kDa)	Apparent mass on the 2DE (kDa)	Mass shift	Injury relation category			Number of fragmented peptides
									Up-regulated	Proteolysis substrate or down-regulated	Fragment	
EF-hand domain-containing 2 (swiprosin-1)	B0K066	Calcium related/ developmental	S	WH	3020	80	27	↓			●	3
EF-hand domain-containing protein D2 (swiprosin-1)	sp|Q4FZY0	Calcium related/ apoptosis/developmental	S	RG	6157	27	29	=		●		6
Elongation factor G 2	O83464	RNA interaction or translation regulator/ cytoskeleton dynamics	S	WH	4897	76	41	↓		●		1
Eukaryotic translation initiation factor 5A-1	C1C496	RNA interaction or translation regulator/ apoptosis	M	WH	3245	17	18	=	●			1
F-actin capping protein beta subunit, putative	B7Q243	Transport/developmental/ cytoskeleton dynamics	S	WH	2200	40	43	=		●		
F-actin capping protein beta subunit, putative	B7Q243	Transport/developmental/ cytoskeleton dynamics	M	WH	2287	40	40	=	●			
Ferritin	Q3HM65	Neuroprotection	M	WH	3197; 3172	20	20	=	●			>8
Ferritin	Q3HM65	Neuroprotection	M	RG	2657; 2681; 2732; 2738; 3737	20	20-22	=		●		>8
Fibronectin-binding protein	UniRef100_ B1QW40	ECM interaction/ Transport/developmental	S	RG	6107	68	33	↓		●		1
FK506-binding protein	Q966Y4	Apoptosis	S	WH	4391	12	10	=	●			3
Gelsolin	B6RB97	Developmental/ Cytoskeleton dynamics	S	RG	6140; 6048	23, 41	59	↑		●		4
Glutathione peroxidase, partial	gi|115926010	Neuroprotection	S	RG	3258	21	28	↑		●		4
Glutathione S-transferase 3	sp|O16116	Neuroprotection	S	RG	3334; 3370	24	27	=		●		2
Heat shock 70 kDa protein 9B (mortalin-2)	D8RYR3	Kinase or kinase regulators/neuroprotection	S	WH	788; 4885	71	79, 89	↑		●		>17
Heat shock cognate 71 kDa protein; Chaperone protein dnaK	A1BET8	Neuroprotection	S	WH	788; 843; 851; 959; 964	69	84, 89	↑		●		>17
Heat shock protein	C1H4I6	Transcription regulator/ factor/neuroprotection	M	WH	3583	79	11	↓		●		1
Heat shock protein 90	D2GZA5	Ups/developmental	S	WH	622; 501; 509	83	94, 99	=/↑		●		>9
Heat shock protein gp96	Q868Z7	RNA interaction or translation regulator/ transport/apoptosis/calcium related	M	WH	594	92	94	=		●		>9
Inositol phosphosphingolipids phospholipase C	C0NSF4	Cytoskeleton dynamics	S	WH	3358	53	23	↓		●		1
IQ motif containing GTPase-activating protein 2	UniRef100_ UPI0000F2C63C	Cytoskeleton dynamics	S	RG	2382	445	49	↓		●		1
Lamin	Q9XZN7	Calpain activity evidences/ cytoskeleton dynamics	M	WH	954	51	81	↑		●		3

Leucine-rich repeat transmembrane neuronal protein 1	A1A4H9	Ups/growth cone and axon guidance/developmental	M	WH	2407; 2388	59	37	↓		●		2
Leucine-rich repeat transmembrane neuronal protein 1	sp|A1A4H9	Growth cone and axon guidance/developmental	M	RG	3749	59	38	↓		●		1
Lin2 protein	P94882	Transcription regulator/factor	S	WH	1166; 1206	16	72–74	↑	●	●		2
Lymphoid-restricted membrane protein	sp|Q12912	Transport	S	RG	5335; 5573	69	8; 9	↓			●	1
Lymphoid-restricted membrane protein	sp|Q12912	Transport	M	RG	3125	69	13	↓			●	2
Lysozyme C	sp|P00698	Neuroprotection	S	RG	4431; 4495; 4576; 4662	14	13; 14	=	●			>6
Lysozyme C	sp|P00698	Neuroprotection	M	RG	2960; 3125; 3757;2862	14	13-17	=	●			>4
Methionyl-tRNA synthetase	Q48LT7	RNA interaction or translation regulator	S	WH	423; 430	75	101	↑		●		2
Novel protein similar to eukaryotic translation initiation factor 5A (Eif5a, zgc:77429)	UniRef100_ Q7ZUP4	RNA interaction or translation regulator/ apoptosis	M	RG	2781	17	19	=	●			1
Nuclear transcription factor Y subunit B-2	Q5QMG3	Transcription regulator/factor	S	WH	1713; 1716	19	53-54	↑		●		2
Nucleolar protein 58	sp|A6ZPE5	RNA interaction or translation regulator	S	RG	2382	57	49	=		●		1
O-sialoglycoprotein endopeptidase	B2GAG0	Endopeptidases or proteases	M	WH	3197	37	20	↓			●	1
Outer membrane protein	C2G0T1	Transport	S	WH	2126; 2352	114	39; 43	↓		●		2
Outer membrane usher protein psaC	Q56983	Transport	S	WH	65; 423	89	101; 284	↑/=		●		2
Oxidoreductase, short chain dehydrogenase/ reductase family	D7HVA7; Q48NP0	Neuroprotection	S	RG	6033	28	33	=		●		1
Peptidyl-prolyl cis-trans isomerase	UniRef100_ A0F006	Kinase or kinase regulators/transcription regulator/folding	S	RG	4040; 4052	17	18-20	=/↓		●		4
Peptidyl-prolyl cis-trans isomerase (Fragment)	UniRef100_ A0F006	Kinase or kinase regulators/transcription regulator/folding	M	RG	3757; 2862	17	16	=	●			3
Peroxidase	Q1VZP2	Neuroprotection	S	RG	3258	24	28	=		●		1
Peroxiredoxin	C4WSM1	Neuroprotection/ developmental	M	WH	2936; 4012; 4016	22	26	=	●			>6
Peroxiredoxin in rubredoxin operon	sp|P23161	Neuroprotection	M	RG	2748	20	26	↑	●			1
Peroxiredoxin-1	P0CB50	Developmental/ neuroprotection	S	WH	3258	22	23	=		●		5
Peroxiredoxin-6	B0WMP0	Neuroprotection	M	WH	2862	24	28	=	●			1
phosphoinositide dependent kinase-1	UPI000192786B	Kinase or kinase regulators/cytoskeletn dynamics	S	WH	4333	88	11	↓			●	1
Polyribonucleotide nucleotidyltransferase	sp|C1DTW6	RNA interaction or translation regulator	S	RG	3177	79	30	↓			●	1

(continued on next page)

Table 1 (*continued*)

Protein name	Accession number	General function	RNC fraction	Regeneration stage	Spot(s)	Predicted mass (kDa)	Apparent mass on the 2DE (kDa)	Mass shift	Injury relation category			Number of fragmented peptides
									Up-regulated	Proteolysis substrate or down-regulated	Fragment	
Polyubiquitin	P62976	Kinase or kinase regulators/ RNA interaction or translation regulator/transcription regulator/factor/UPS	S	WH	4850	9	7	=	●			2
Prefoldin subunit alpha	Q6LX82	Neuroprotection	S	WH	1162	16	74	↑		●		1
Pre-mRNA cleavage factor	A7URJ4	RNA interaction or translation regulator	S	RG	6062	16	33	↑		●		1
Pre-mRNA-processing ATP-dependent RNA helicase PRP5	sp|Q6FML5	RNA interaction or translation regulator	S	RG	5583; 5522	92	8; 9	↓			●	2
Proteasome subunit alpha	O59219	UPS	S	WH	4109	29	12	↓			●	1
Proteasome subunit beta type	Q1HPR0	UPS	M	WH	2817	23	29	↑	●			1
Protein grpE	Q14LB5	Neuroprotection	S	WH	1623	24	57	↑		●		1
Putative ankyrin repeat protein L675	Q5UNU1	Growth cone and axon guidance	S	WH	662	54	93	↑		●		1
ras homolog gene family, member A	UPI0001C65337	Kinase or kinase regulators/ RNA interaction or translation regulator/transcription regulator/factor/transport/ calcium related/apoptosis/ developmental/ neuroprotection	S	WH	3098	21	25	=		●		1
Ras-related protein Rab-11A	Q2TA29	Transport//cytoskeleton dynamics	M	WH	2692; 2731; 2759; 2837	24	28-31	=/↑	●			8
Ras-related protein Rab-11A	sp|Q2TA29	Transport/cytoskeleton dynamics	M	RG	2357	24	28	=	●			1
Ras-related protein Rab-15	sp|Q1RMR4	Transport/cytoskeleton dynamics	M	RG	2307; 2345; 2748; 3766	21-25	26-29	↑/=	●			4
Ras-related protein Rab-6A	A0CE65	Transport/cytoskeleton dynamics	M	WH	3313; 2848; 2837; 2759; 2817; 2894	23-25	16-30	↑/=/↓	●		●	
Ras-related protein Rab-7a	sp|Q3T0F5	Transport/cytoskeleton dynamics	M	RG	2417	24	27	=	●			1
Regulatory protein Crp	D8J4J6	Transcription regulator	S	RG	1786; 4431	28	14; 66	↑/↓		●	●	2
Regulatory protein Crp	D8J4J8	Transcription regulator	S	RG	6142	18	45	↑		●		1
Regulatory protein Crp	D8J4J7	Transcription regulator	S	RG	5504	63	9	↓			●	1
Rho1 GTPase	115963593	Kinase or kinase regulators/RNA interaction or translation regulator/transcription regulator/factor/transport/ calcium related/apoptosis/ developmental/ neuroprotection/ cytoskeleton dynamics	S	WH	3098	23	25	=		●		3
Rho-type GTPase-activating protein 2	Q10164	Cytoskeleton dynamics	S	WH	103; 557	144	200; 95	↑/↓		●	●	3

RNA binding motif (Fragment)	Q13377	RNA interaction or translation regulator	S	RG	6103	56	39	↓	●		2
RNA ligase	E3KDA7	RNA interaction or translation regulator	S	WH	1147; 1159; 1165; 1166	107	74–75	↓	●		4
RNA polymerase sigma factor sigI	E0U2K8	Transcription regulator/ factor/neuroprotection	M	WH	2445	29	36	↑	●		1
Serine/threonine-protein kinase ATM	sp|Q9M3G7	Kinase or kinase regulators/transcription regulator/developmental/ neuroprotection	S	RG	6030	435	32	↓	●		1
Severin	Q24800	Cytoskeleton dynamics	S	WH	4880	42	43	=	●		1
Signal transduction histidine kinase	C5SFK7	Kinase or kinase regulators	S	WH	634	37	93	↑	●		2
Signal transduction histidine kinase	C5SFK7	Kinase or kinase regulators	M	WH	523; 530	37	97	↑	●		1
Spectrin	115920116	Calpain activity evidences/ growth cone and axon guidance/developmental/ cytoskeleton dynamics	M	WH	235; 659	279	92; 162	↓	●		6
Spectrin	UPI00015B61A3	Calpain activity evidences/ cytoskeleton dynamics	S	RG	971; 3760	279	21; 94	↓	●	●	2
Spectrin alpha chain	115954248	Calpain activity evidences/ growth cone and axon guidance/developmental/ cytoskeleton dynamics	S	WH	103; 217; 541; 551; 557; 4884	279	43-200	↓	●	●	>7
Spectrin beta chain	B0WDS4	Calpain activity evidences/ cytoskeleton dynamics/ lipid metabolism and transport	S	RG	4969; 5202	266	10; 11	↓		●	2
Spectrin beta-G	Q9U9J8	Calpain activity evidences/ growth cone and axon guidance/developmental/ cytoskeleton dynamics	S	WH	541; 551; 730	267–272	93–97	↓	●	●	3
Spectrin beta-like	UPI0001D39591	Calpain activity evidences/growth cone and axon guidance/ developmental/ cytoskeleton dynamics	S	WH	730	272	93	↓		●	1
START domain-containing protein	A9ZT01	Cytoskeleton dynamics/ developmental	S	WH	1153; 1269; 1286; 1660	43	55; 70; 75	↑	●		>7
START domain-containing protein (Fragment)	A9ZT01	Developmental/ cytoskeleton dynamics	S	RG	1657; 1668; 1678	43	69; 70	↑	●		>4
Synaptosomal-associated protein 25	sp|P36976	Transport/growth cone and axon guidance/ calcium related/ cytoskeleton dynamics	M	RG	2118	24	33	↑	●		1
Transcription factor Sox-12	sp|Q8AXQ4	Transcription regulator/ apoptosis/developmental	S	RG	5225	27	10	↓		●	1
Transcriptional activator Rgg/GadR/MutR	D0AHM2	Transcription regulator	S	RG	2546; 5583	39	8; 47	=/↓	●	●	2
Transcriptional regulator, LacI family	Q03ZF8	Transcription regulator/factor	S	WH	65	35	284	↑	●		1

(continued on next page)

Table 1 (*continued*)

Protein name	Accession number	General function	RNC fraction	Regeneration stage	Spot(s)	Predicted mass (kDa)	Apparent mass on the 2DE (kDa)	Mass shift	Injury relation category			Number of fragmented peptides
									Up-regulated	Proteolysis substrate or down-regulated	Fragment	
tRNA (guanine-N(1)-)-methyltransferase	Q4WXA1	RNA interaction or translation regulator	S	WH	1108; 1109; 1110; 1120; 172	44	109; 77	↑		●		4
tRNA pseudouridine synthase A	D9WR76	RNA interaction or translation regulator	S	WH	2735	31	31	=	●			1
Tubulin alpha chain	P53372	Cytoskeleton dynamics	S	WH	1138; 1301; 1153; 1282; 1290; 4207; 4574; 1300	28; 50	76	↑/↓		●	●	>16
Tubulin alpha-1D chain	Q2HJ86	Cytoskeleton dynamics	M	WH	3022	50	25	↓			●	>9
Tubulin beta chain	P11833	Cytoskeleton dynamics	S	WH	1300	50	69	↑		●		>15
Tubulin beta-2C chain	Q3MHM5	Cytoskeleton dynamics	M	WH	3810	50	8	↓		●		3
Tubulin alpha	Q2HJB8	Cytoskeleton dynamics	M	WH	3497; 4012; 2894	50	13; 26; 27	↓			●	>3
two-component LuxR family transcriptional regulator	UPI0001DD0746	Transcription regulator/factor	M	WH	161; 142; 146; 162	24	200	↑		●		4
Two-component system sensor histidine kinase/response regulator hybrid	D7JXA2	Kinase or kinase regulators/transcription regulator/factor	S	WH	4744	156	8	↓			●	1
ubiquitin C, partial	UPI0001926211	Transcription regulator/factor/ups/apoptosis/growth cone and axon guidance	S	WH	4850	9	7	=	●			**3**
Ubiquitin family protein	A8IS91	Transcription regulator/factor/ups/apoptosis/growth cone and axon guidance	S	WH	4574	9	9	=	●			1

Ubiquitin/actin fusion protein	gi|115918029	UPS	S	RG	654; 853; 857; 1867; 1971; 1994; 2041; 2051; 2069; 2382; 3760; 4047; 4385; 4588; 4901; 4966; 4969; 5088; 5198; 5217; 5522; 5583; 6042; 6048; 6091; 6112; 6140	42	8–21; 49–63; 116–187	↑/=/↓		●	●	>15
Ubiquitin-conjugating enzyme	sp|Q1RMX2	UPS	S	RG	4306; 4198	16–17	15–16	=		●		2
Villin 2	UPI0000D8B3D9	Cytoskeleton dynamics	S	WH	818; 1031; 1032	68	82–88	↑		●		3
Villin-1	Q29261	Cytoskeleton dynamics	S	WH	577	15	95	↑		●		1
von Hippel-Lindau binding protein 1-like	UPI0001CBB031	Neuroprotection	S	WH	3020	21	27	↑	●			1
V-type proton ATPase catalytic subunit A	C3XZE0	Calcium related/ neuroprotection	S	RG	5088; 6130	68	11; 80	↑/↓			●	5
*Similar to 26S protease regulatory subunit	115942106	RNA interaction or translation regulator/ transcription regulator/ factor/ups	M	WH	1588	45	144	↑		●		3
*Similar to ankyrin repeat protein	A2FHV3	Growth cone and axon guidance	S	WH	1269; 1286	72	70	=		●		2
*Similar to Dihydropyrimidinase	UPI0001925E76	Developmental	M	WH	1056	32	77	↑		●		1
*Similar to Dihydropyrimidinase	UPI0001925E76	Developmental	S	WH	1110	32	77	↑		●		1
*Similar to fibronectin type III domain-containing protein	A8F5G5	ECM interaction/ transport/developmental	S	RG	2656	174	40	↓		●		**1**
*Similar to LacI family transcription regulator	C0A988	Transcription regulator	S	RG	2934	41	34	↓		●		1
*Similar to luminal binding protein	C5YNI7	Neuroprotection	S	WH	788	16	89	↑		●		1
*Similar to peroxiredoxin V protein	B3RM02	Neuroprotection	S	RG	3993; 6076	20	17–18	=		●		4
*Similar to Rhs family protein	UniRef100_ A7VY20	Kinase or kinase regulators/ Neuroprotection	S	RG	1842	275	64	↓		●		1
*Similar to ubiquitin specific peptidase 36	B7PMA2	UPS	S	WH	1159; 1165	127	74–75	↓		●		2

control (CNT) and the regenerating (WH/RG) groups as described below:

Fragments: if presenting a decreased mass and if the correspondent relative spot volume in the WH/RG group was superior to the CNT group;
Proteolysis substrates/down-regulated: All mass shift categories that presented a correspondent relative spot volume in the WH/RG group inferior to the CNT group, as there is no possible way to distinguish proteins that are being down-regulated or are just being degraded through proteolytic pathways;
Up-regulated proteins: If presenting an increased or equal mass and the relative spot volume in the WH/RG group is higher than in the CNT group (the only subset of proteins that could not be explained by any proteolytic events).

Fig. 3 presents the number of identified proteins included in each category (related with proteolytic events or up-regulated) with the correspondent mass shifts (No mass shift, increased mass and decreased mass) for the WH and RG events. In the WH RNC soluble fraction, 94% of the identified proteins were related to proteolytic/down-regulated events (79% of the proteins were considered as proteolysis substrates/down-regulated; and 15% were fragments of the identified proteins). Only 6% of the identified protein spots could be assigned to the up-regulated proteins (Table 1; Supplementary Table 2). In the RNC membrane fraction, a lesser extent of the identified proteins was involved in the proteolytic pathways (75% of which, 45 proteins were categorized as proteolysis substrates and 12 as being fragments). The remaining proteins were considered to be up-regulated (25%) (Supplementary Table 2).

The proteome of the re-growing nerves (RG) was compared with the correspondent control and a total of 202 spots throughout both subcellular fractions were found to have significant changes in terms of relative spot volumes. Nevertheless, still a high number of proteins were either identified as proteolysis substrates/down-regulated or as fragments (177 proteins in the soluble fraction and 53 proteins in the membrane fraction), highlighting the importance of proteolytic pathways that persist throughout RNC re-growth stage, although in lower levels than in WH stages. Also, similarly to the results obtained in the WH events, only 5% of the proteins were up-regulated in the soluble fraction of the RG RNC and 19% in the membrane fraction of the RG RNC (Supplementary Table 4).

In several cases, the same protein was identified in multiple spots excised from substantially different positions on the 2DE gels, and consequently the same protein was found in the different established categories (Fig. 4). This ubiquitous distribution of some proteins throughout the 2DE gels is probably due to several cleavage events, and in some cases associated with certain proteolytic pathways. The existence of the same protein in various M forms was also previously reported in a similar study using 2DE proteomics to study injury effects on regenerating mollusk neurons [35,37]; which was the case for actin, tubulin, ATP synthase, phosphoglycerate kinase, HSP70, arginine kinase, enolase, an actin modulator — arp2/3, results that are all in agreement to molecular mass shifts found in the injured starfish RNC. Additionally, several spots were identified with more than one protein, most probably due to the above-described abundance of proteolysis products.

4. Discussion

4.1. *Proteolysis as a post-translational modification*

Post-translation modifications such as phosphorylation are well established signaling events in neural injury, and for this reason it is not surprising to find indications of these processes in the regenerating starfish RNC [5]. Even though proteolytic pathways are recognized for their role both in normal [56] and regenerating neurons [22], this subject has been given quite less consideration than protein synthesis. The occurrence of

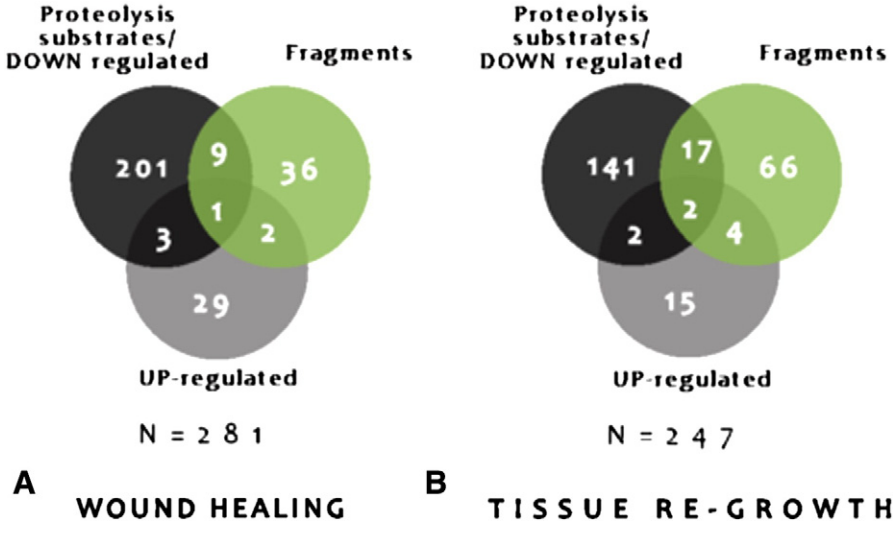

Fig. 4 – Protein distribution according to their injury relation in both soluble and membrane fractions (up-regulated; proteolysis substrate/down-regulated or proteolysis fragment) for wound healing (A) and re-growth (B) radial nerve cord events.

proteolytic events in such great extent suggests that the starfish RNC regeneration depends on the occurrence of such processes simultaneously with protein synthesis.

During arm tip wound healing events, a great involvement of the proteolytic pathways is expected, leading to major ECM reorganizations necessary for tissue remodeling, a process that has already been described to occur during intestine regeneration of a sea cucumber specie [7,8,33]. Within a regenerating nervous system, the proteolytic pathways are also expected to be involved soon after injury, affecting especially cytoskeleton proteins in order to promote the correct formation of axonal growth cones [57].

Herein we describe the pathways that were found to be regulated through proteolysis, and greater emphasis is given to the proteolytic pathways and their protein substrates. The roles of the few proteins that were identified as up-regulated during starfish RNC regeneration events are also discussed.

A detailed description of the identified proteins and their related functions within neural regeneration events is here presented as a hypothesis-generating work, aiming to clarify the signaling functions of the newly generated protein fragments. The list of identified proteins in RNC WH and RG events with the corresponding annotations for generalized function and injury related category can be found in a summarized form in Table 1, or with the complete set of information in Supplementary Tables 2 and 4.

4.2. *Cytoskeleton dynamics is modulated through de novo protein synthesis and proteolysis in the regenerating radial nerve cord*

4.2.1. *Actin and microtubule regulating proteins*

Neural regeneration, axon guidance and growth, requires spatial and dynamic reorganization of the cytoskeleton. Neurons extend axons towards appropriate targets in the regenerating nervous systems via growth cones, the motile structures at axonal tips. The growth cone, a highly motile cellular compartment at the tips of growing axons, is composed by a central region filled with organelles and microtubules and a peripheral, highly dynamic, actin-rich region containing lamellipodia and filopodia [58] (Fig. 5). Highly tuned actin filament organization within the growth cone dictates the permissive protrusion of newly formed microtubules influencing the axon growth [59]. The actin turnover dynamics is regulated by actin nucleating, severing, branching and bundling proteins. The Rho GTPases Cdc42, Rac and Rho, are key regulators of the cytoskeleton, and therefore are also implicated in these processes (reviewed in [60]) driving many of the required morphological changes during axogenesis and axonal regeneration. Dynamic cytoskeleton remodeling events are also vital for cells at the injury site to undergo a morphallactic process and achieve functional re-growth of the lost tissues. Since this cellular strategy causes loss of

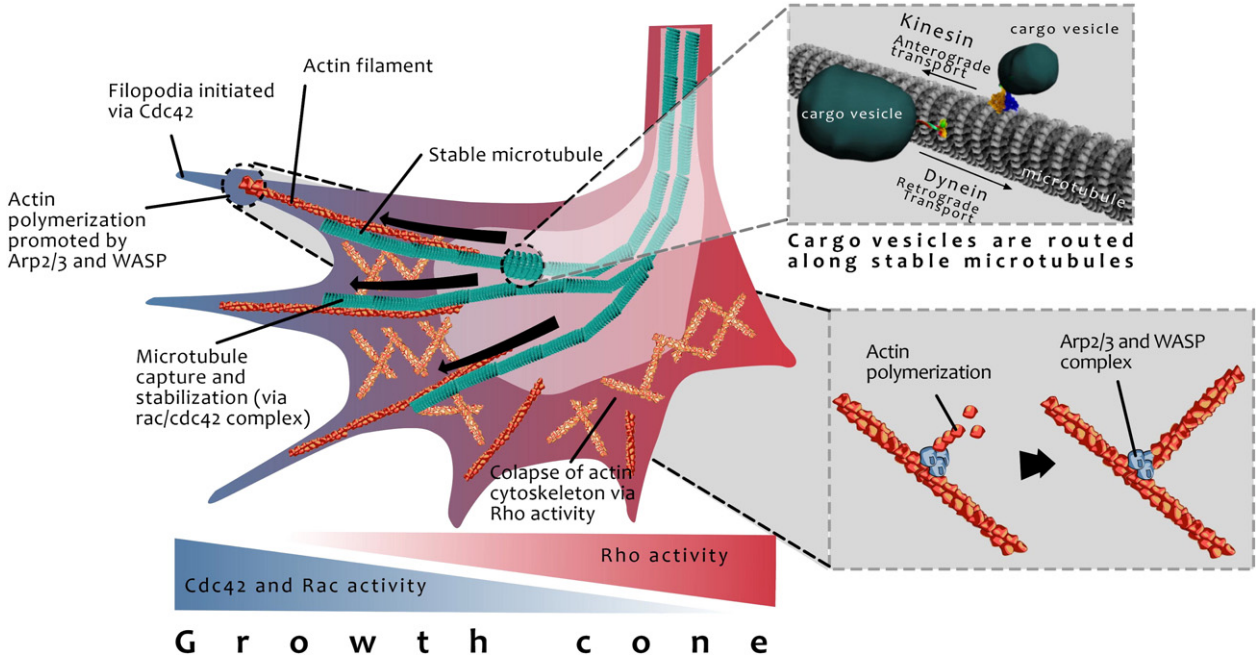

Fig. 5 – Neurons extend axons towards appropriate targets in the regenerating nervous systems via growth cones, the motile structures at axonal tips. The Rho family of GTPases, including Cdc42, Rac and Rho, regulate the dynamics of actin microfilaments and microtubules, and have been implicated in growth cone steering by molecular gradients [96]. Cdc42 activation in growth cones stimulates formation of dynamic, finger-like filopodia [97] comprising bundles of actin microfilaments. In addition to their roles in modulating microfilaments, Rho GTPases affect microtubules, which then affect neuronal growth [98]. This illustration represents a hypothetical mechanism by which Rho GTPases mediate growth cone steering. The concentrations of active Rac and Cdc42 (red) are relatively high on the right side of the growth cone promoting filopodia formation, but Rho activity (blue) is relatively low on that side. Conversely, active Rho is relatively high on the left side and active Rac and Cdc42 are low resulting on filopodial collapse, forming lamellipodia instead (Figure based on [99]).

tissue specificity in which terminally differentiated cells become undifferentiated (i.e., dedifferentiation) and then again to re-differentiate into a cell of a different lineage (i.e., trans-differentiation), it is expected that highly coordinated cytoskeleton rearrangements take place for such a dramatic cell morphology change.

Similarly to other results obtained in proteomic studies of regenerating animal models [29,30] several actin and microtubule regulators were found to be up-regulated in *M. glacialis* WH RNC namely, Rab-11A, Rab-6, F-actin capping protein beta subunit, the small GTPase Cdc42 and actin-related protein 2/3 complex subunit 5 (arp 2/3). The last two proteins, are known to be key effectors of the Wiskott–Aldrich syndrome protein (WASP) family verprolin-homologous protein (WAVE) pathway, which induces cytoskeletal changes by promoting actin polymerization by direct interaction with arp 2/3 complex and profilin promoting axon growth [61] by regulating filopodia formation [62]. It was further proved by Garvalov and colleagues [63] using Cdc42-null neurons that this GTPase acts upstream of a local actin depolymerizing activity, which is required for initial axon formation and hence, the up-regulation of these proteins during starfish RNC regeneration events is expected. Conversely to arp 2/3 or Cdc42, increased Rho activity prevents neurite initiation and induces neurite retraction [64]. The inactivation of Rho appears to be regulated by several mechanisms; namely by the Rho GTPase-activating protein, which enhances the intrinsic rate of GTP hydrolysis of Rho, suppressing Rho activity during neurite formation. Rho-type GTPase-activating protein 2 and Rho1 GTPase were also identified in the WH RNC in different protein forms: 1) the Rho-type GTPase-activating protein 2 was identified with an apparent M above the expected and also, as a proteolytic fragment, indicating that this protein is being targeted to proteolysis probably through the ubiquitin/proteasome pathway, which is in agreement with previous reports relating the down-regulation of Rho activity due to targeted degradation mediated by the UPS system [65]; 2) Rho1 GTPase was identified in spots with the expected M, however having a reduced spot volume relatively to controls, caused either by a down-regulation or targeted proteolysis.

Not surprisingly, actin itself was identified in a multitude of different 2DE spots and consequently was one of the proteins that appeared to be regulated at two levels (Supplementary Fig. 3): 1) by an increase in protein levels (up-regulation) in WH RNC, indicating that in this early stage of regeneration actin is being *de novo* synthesized; 2) and by targeted proteolysis in both WH and RG RNC (identified as fragment and as proteolysis substrate). This suggests that the several actin forms are extremely dynamic and precisely controlled by different pathways. The microtubule regulator, Rab-6A is also an example of modulation at different levels, being identified in WH RNC with increased, no change and decreased apparent M and, as being up-regulated or a fragment (Supplementary Table 2).

Furthermore, actin-binding proteins, such as villin and severin, were also identified in WH RNC. These are known to promote the bundling, nucleation, capping and severing of actin filaments. Both proteins were identified as proteolytic fragment or down-regulated, thus suggesting that proteolysis might regulate the activity of these actin-binding proteins to promote actin filaments polymerization or depolymerization in WH starfish RNC. Several proteolytic fragments of calmodulin were also identified in the WH RNC, a protein known to regulate actin-based motility and to participate in the signaling pathways used to steer growth cones [66].

Similarly to WH, several GTPases were also identified in the RG RNC. Among these are the GTPases Rab-11A, Rab-15 and Rab-7A that were identified in several spots and up-regulated, which is in agreement with results obtained in other studies [29]. Several other proteins involved in actin and microtubule regulation were identified in the RG nerve namely, IQ motif containing GTPase-activating protein (proteolysis substrate/down-regulated) and the ATP-binding cassette sub-family A member 7 (proteolysis substrate/down-regulated), both involved in the Cdc42 protein signal transduction events [67]. Profilin, an actin-binding protein involved in restructuring of actin cytoskeleton, was only identified in RG RNC as being up-regulated and also as a proteolysis substrate. Once more, these facts suggest that *de novo* protein synthesis and proteolytic pathways regulate actin dynamics, resulting in cytoskeleton changes associated with growth cone extension/retraction or, cellular transdifferentiation processes. Also involved in actin filament formation is the allograft inflammatory factor [68], which was also up-regulated in the RG RNC. This protein might be promoting actin polymerization towards the formation of microfilaments from the newly synthesized actin monomers, while other cytoskeleton proteins are being cleaved, as expected, according to the above explained. Other actin bundling proteins were also identified namely, alpha-actinin-1 (proteolytic fragment), gelsolin (proteolytic fragment/down-regulated), and calmodulin (up-regulated and proteolytic fragment).

These results seem to indicate that several pathways that govern cytoskeleton dynamics are oriented towards neural re-growth as soon as 48 h post-arm tip ablation. Nevertheless, it has to be considered that the majority of protein regulation at the post-translational level is extremely dependent on the physical location in the cell where the target proteins need to exert their actions, or be inactivated/eliminated. Hence, opposite modifications may be occurring in different axonal locations, creating an endeavor task to interpret the function of a particular protein in a particular "proteolytic" state. For this reason, most of the results henceforward will be discussed in terms of being regulated or not, by proteolytic pathways, for whose the particular function of the regulation still remains to be clarified.

4.2.2. Calpain protease remains active throughout the course of regeneration

One of the proposed functions for calpain mediated cytoskeleton rearrangements relies in the proteolytic cleavage of spectrin, the protein that through its binding partner ankyrin, connects many integral membrane proteins to the actin cytoskeleton [69]. This process was suggested to facilitate membrane fusion of axoplasmic vesicles, helping the construction of the growth cone or extension of the axon (Fig. 6) [23]. Calpain phosphorylation has been previously reported in regenerating RNC of *M. glacialis* suggesting that its proteolytic activity is modulated through phosphorylation [5]. Also, in the same study spectrin was found to be dephosphorylated only

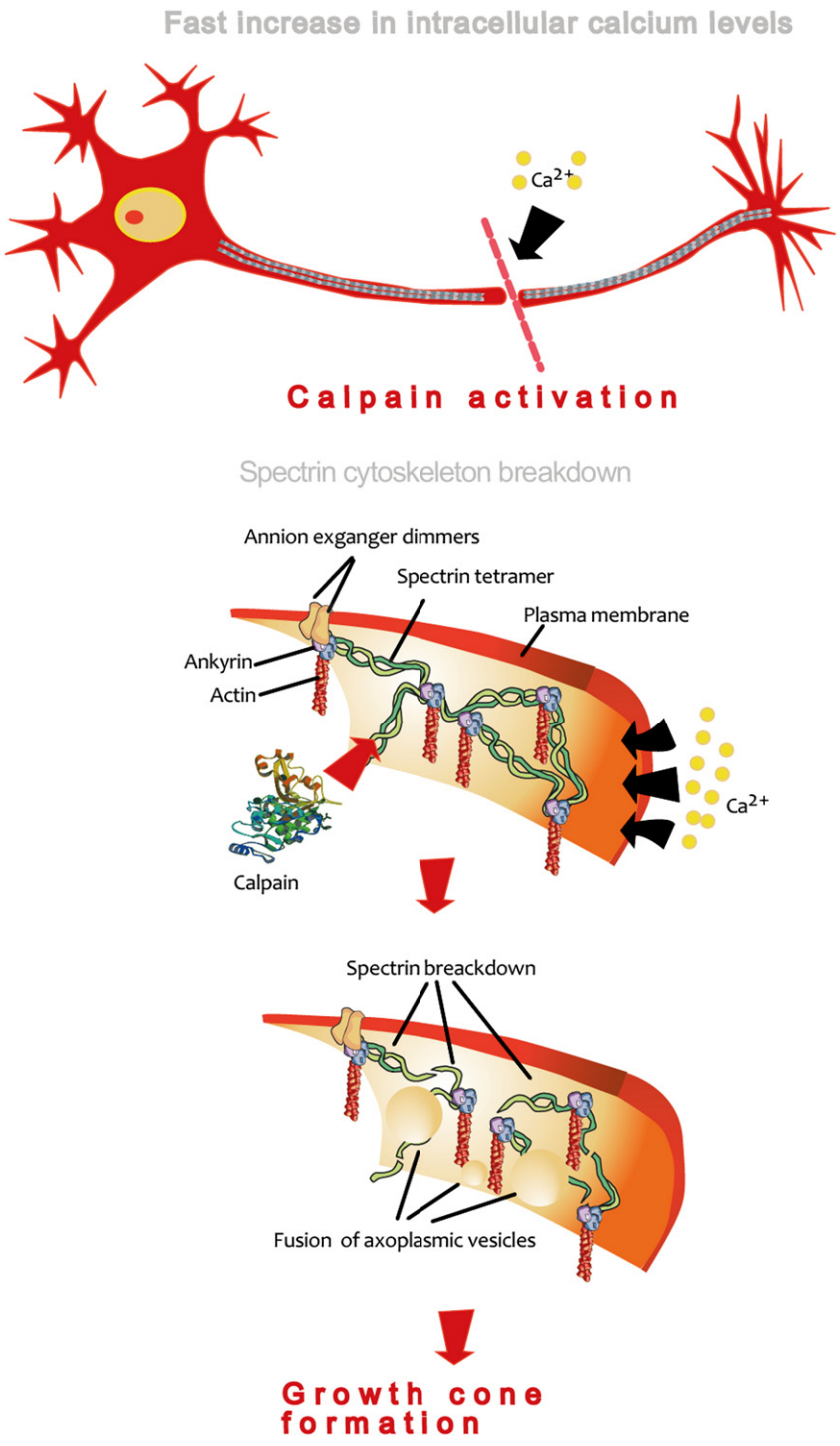

Fig. 6 – As a result of neuronal injury, intracellular calcium concentration rises rapidly causing the activation of calcium-dependent proteases, such as calpain, which in turn carries out the process of protein degradation necessary for successful regeneration, that include proteolysis of the membrane associated cytoskeletal component spectrin.

in regenerating RNC suggesting that like in other organisms, a dephosphorylation step associated with the cascade of injury signaling events is critical for calpain mediated proteolysis of spectrin during echinoderm RNC [5]. In the present study also several fragments of spectrin like proteins (Supplementary Fig. 4), and of its binding partner ankyrin, were identified in the WH RNC, indicating calpain involvement in starfish RNC early regenerating events.

In the RG RNC DIGE gels, seven different protein spots, ranking from 11 to 94 kDa, were also identified as spectrin (6 spots) and ankyrin (1 spot), which seems to indicate that calpain mediated proteolysis is not only present in the initial

WH stages, but it seems also to be critical for nerve re-growth. It is also possible that, the axon guidance function of spectrin may be attributed only to the fragments generated by the subsequent proteolytic events, since spectrin is ubiquitously distributed in cells and therefore might not always be exerting its function as a guidance molecule. Spectrin is also known to bind to the actin-related protein subunit of the motor transport protein dynein [70]. Hence, the on-going proteolytic events that persisted throughout RNC RG may be shaping the tracks of the vesicular transport within starfish nerve regeneration events. In fact, the supply and concentration of vesicles at restricted sites along the injured axon are known to be one of the critical steps, which enable subsequent nerve fiber elongation after growth cone formation [71].

Since at the RG stage the axonal membranes are properly sealed, the intracellular calcium levels are restored and thus, other pathways may be responsible for calpain activation and regulation during nerve elongation. This might involve other calcium regulating proteins or additional post-translational modifications. In fact, several proteins known to regulate intracellular levels of calcium were identified in RG RNC which include V-type proton ATPase catalytic subunit A (proteolysis substrate/down-regulated and fragment), and several calcium binding proteins such as calmodulin.

4.2.3. *Ubiquitin proteasome system (UPS) is actively involved in regulating protein levels throughout the radial nerve cord regeneration events*

Another key intervenient in the proteolytic events necessary for cytoskeleton remodeling is the ubiquitin–proteasome system (UPS). The current hypothesis on the UPS role within regeneration events is related with the targeted degradation of cytoskeletal components and microtubule rearrangements [72]. Recently, using yeast as model, it was suggested that proteasomal mediated degradation resolves the competition between cell polarization and wound healing through the dispersion of polarity factors enabling targeting of repair factors to the site of damage [73]. Although additional studies using multicellular organisms are still sought, the possibility remains that the UPS system might have the same function in regulating neuronal polarization during regeneration.

Several components of the UPS system were identified in the WH RNC: the proteasome subunit alpha (as a proteolysis substrate/down-regulated or as a fragment) and beta (as up-regulated); three different spots were identified with ubiquitin like molecules and all up-regulated, which correlates with the recycling of ubiquitin via UPS; the 26S protease regulatory subunit (which was identified with an increased mass and as a proteolysis substrate/down-regulated); and a ubiquitin specific peptidase 36 (proteolysis substrate/down-regulated). The latter belongs to the large family of deubiquitinating proteases that in addition to ubiquitin recycling are involved in processing of ubiquitin precursors; proofreading of protein ubiquitination and disassembly of inhibitory ubiquitin chains [74].

Additionally, both actin and tubulin were identified as proteolysis substrates or as fragments, most probably by the UPS proteolytic pathways.

Furthermore, several proteins were identified with apparent M above the expected along with the identification of the respective proteolytic fragments. This might indicate that these proteins are being conjugated with ubiquitin for targeted proteolysis by the proteasome system. Some examples occurring in WH RNC are: the hypothetical protein BH2562, and Rho-type GTPase-activating protein 2.

Moreover, similarly to WH RNC, during RG events a multitude of spots were identified as being either actin or tubulin with considerably different M, decreased spot volumes in comparison with controls and also as fragments. For 23 protein spots, proteolytic fragments of an ubiquitin/actin fusion protein were identified (Supplementary Fig. 5); reinforcing the hypothesis that cytoskeleton degradation towards RNC re-growth is being regulated by several protein degradation pathways. This was further strengthened by the identification of an ubiquitin-conjugating enzyme (proteolysis fragment or down-regulated), which was not identified in WH RNC gels.

4.3. *Vesicular transport*

Small GTPases, besides being key effectors in the regulation of cytoskeleton and microtubule dynamics, are also known to be involved in the delivery of proteins and lipids to the axon, through the exocytic machinery (anterograde transport), as well as in the internalization of membrane and proteins at the leading edge of the axon, by endocytosis (retrograde transport) [60]. Therefore, the previously mentioned GTPases, identified in WH and RG RNC gels can also be involved in axonal vesicular transport.

The synaptosomal-associated protein 25 (SNAP-25) was also identified with a decreased spot volume however, only in RG RNC. SNAP-25 is known to associate with proteins involved in vesicle docking and membrane fusion, also previously described to be regulated by proteolytic events [75]. SNAP-25 cleavage inhibits growth cone extension [76], and its mRNA has been reported to be enriched in embryonic axons [22]. Other proteins involved in vesicle targeting and fusion were also identified namely, lymphoid-restricted membrane protein, identified as a fragment in both soluble and membrane fractions of RG RNC.

4.3.1. *Other axon guidance and growth cone regulator proteins modulated by proteolysis*

During re-growth of the axons post-axotomy, the growth cone navigates a series of choice points to find the appropriate targets. These guidance decisions are shaped by a balance of attractive and repulsive cues found in the extracellular environment, that can act locally or at a distance [77]. The question of how guidance receptors and their downstream effectors are targeted to, and distributed within functional domains of the growth cone plasma membrane, remains unanswered, even though it consists of an important key to understand the mechanisms of axon path finding.

Several proteins with known functions in axon guidance were identified and seem to maintain their function throughout both regeneration stages (WH and RG). This is the case for: the leucine-rich repeat transmembrane neuronal protein 1, which has been previously reported to participate in axon guidance by acting as midline repellent for commissural axons through the Robo (Roundabout) receptor [78,79]; and the EF-hand domain-containing protein D2 (swiprosin-1), a protein that regulates the formation of neuron projection development.

In opposition, several proteins were only identified in one of the studied regeneration stages, highlighting a probable shift in the axon guidance molecules needed for RNC WH and RG events. This is the case for dihydropyrimidinase (increased mass and categorized as proteolysis substrate), which was identified in several different spots only in WH events, and is known to be involved in the semaphorins signaling pathway, necessary for cytoskeleton remodeling [80].

4.3.2. Protein synthesis machinery and RNA transport

Translation of mRNAs in injured axons provides a locally renewable source of proteins at sites that may be thousands of micrometers apart from the neuronal cell body, and hence, are essential for the rapid initiation of regenerative responses. For this reason it is not surprising to identify several ribosomal proteins in the WH RNC, which is in agreement with other proteomic studies on regeneration events [29], namely 40S ribosomal protein S21 (up-regulated) and 30S ribosomal protein S21 (proteolytic fragment). In addition, the elongation factor G2 was also identified (proteolytic fragment) as well as the ras homolog gene family, member A and Rho1 GTPase, both regulators of translation, also identified as proteolysis substrates.

However, several ribosomal proteins were still altered (in terms of spot volume) in RG RNC namely, the 40S ribosomal protein S21 (up-regulated); 30S ribosomal protein S8, 50S ribosomal protein and 54S ribosomal protein L4, identified as proteolysis substrate or as fragments; and a protein similar to eukaryotic translation initiation factor 5A, identified as being up-regulated.

Several proteins that assist the folding process of *de novo* synthesized proteins were also identified in the WH RNC, namely, calreticulin. This protein interacts with nascent proteins in the endoplasmic reticulum along with disulfide-isomerase A3 [81], which was also identified in WH RNC. Several other folding assistant proteins were identified namely, chaperonin containing TCP1 subunit 5 (epsilon), several heat shock proteins, prefoldin subunit alpha, protein grpE and luminal binding protein. All these folding assistants presented a decreased spot volume during WH due to down-regulation or proteolytic cleavage. The only up-regulated proteins with chaperone functions identified in the WH RNC were von Hippel–Lindau binding protein 1-like and a putative FK506-binding protein, the last being known to stabilize newly synthesized proteins by preventing its proteasomal degradation [82].

The number of proteins that act as folding assistants was substantially reduced in the RG RNC when compared with the WH events, being limited to the identification of a chaperone protein htpG (proteolysis substrate/down-regulated) and a peptidyl-prolyl cis-trans isomerase (up-regulated). These observations further suggest that proteolysis might also control local protein *de novo* synthesis machinery in starfish RNC.

RNA localization is a highly regulated process that requires mechanisms for selecting which mRNAs to target for transport in distal neuronal processes. The mRNAs encoding axonally synthetized proteins must be delivered to the axonal compartment to enable local translational regulation, a strategy used by neurons to modulate protein levels in distal processes upon stimulus (reviewed in [23,24]). mRNAs to be transported are complexed with multiple proteins to form a ribonucleoprotein (RNP), that either engages with microtubule motor proteins for long range transport along the axon or, with microfilaments for short distances displacement. However, knowledge of what RNPs are needed for localization, how their activity is regulated, and what sequence structures are recognized, is rather sparse. Several proteins that are involved in RNA modification and RNA binding were identified in WH RNC events such as, tRNA pseudouridine synthase A (up-regulated); tRNA (guanine-N(1)-)-methyltransferase, RNA polymerase sigma factor sigI, RNA ligase, methionyl-tRNA synthetase, identified as proteolysis substrates/down-regulated, and other cases like the cysteinyl-tRNA synthetase identified as proteolytic fragments. In the RG events also several proteins that are involved in RNA modification were identified, these include: the nucleolar protein 58 (proteolysis substrates/down-regulated), a protein that is necessary for the formation of the large protein complexes that aggregate to RNA (RNP complexes) and enable its transport by engaging with motor proteins or microtubules; polyribonucleotide nucleotidyltransferase, involved in RNA degradation and identified as a fragment; pre-mRNA cleavage factor (proteolysis substrates/down-regulated); pre-mRNA-processing ATP-dependent RNA helicase PRP5 (fragment); and RNA binding motif (proteolysis substrates/down-regulated) among others.

Once more, proteolysis seems to be having an important but yet, unknown role in RNA regulation during RNC regeneration events. Further studies in echinoderm species are needed to understand the dynamics of mRNA axonal transport during regeneration.

4.3.3. Kinases and transcription factors

Axonal injury induces local activation and retrograde transport of several mitogen-activated protein kinases (MAPK), including Erk [36] and the c-Jun N-terminal kinase (JNK) [24]. These two activated kinases, then interact with the motor proteins dynein and dynactin, engaging in the neuronal retrograde transport system back to the neuron body, where they exert their functions as injury signals. However the transport of such signals is a complex process since many of these kinases are activated by reversible phosphorylation, thus further protection against phosphatases is needed throughout the journey to the neuronal body. As previously stated, activated Erk interacts with the calpain proteolytic fragment of vimentin, which further protects it from dephosphorylation before reaching the cell body [37]. Cdc42, a small GTPase, is one of the intervenients of the JNK cascade identified as being up-regulated in the WH RNC events. In addition, a fragment of a protein homologous to the dynein motor protein, the axonemal 84 kDa protein, was also found in the WH RNC. Several other kinases without previous relation with regeneration processes were also identified, namely two-component system sensor histidine kinase/response regulator hybrid, signal transduction histidine kinase among others.

Similarly, a number of kinases were also identified in the RG RNC, i.e., cGMP-dependent protein kinase (proteolysis substrates/down-regulated); Rhs family protein (proteolysis substrates/down-regulated) and serine/threonine-protein kinase ATM (proteolysis substrate/down-regulated), along with several others. Although the relation with proteolytic events is not clear, it can be a way to modulate these particular kinases and hence the correspondent downstream events.

Axonal injury also activates several transcription factors that are also translocated back to the nucleus [83]. Several transcription factors were identified in the WH RNC, such as the Cat eye syndrome critical region protein 2 (Cecr2) (proteolysis substrates/down-regulated), which is particularly interesting given its predominant expression in neural tissues during neurulation, as well as in the intermediate zone of the spinal cord, suggesting that it may play a role in neuronal development [84]. However, this study is the first to associate Cecr2 to neuronal regeneration events. Also in WH RNC the transcriptional regulator LacI family, two-component LuxR family transcriptional regulator, lin2 protein (up-regulated and proteolysis substrates/down-regulated) and nuclear transcription factor Y subunit B-2 were all identified with apparent masses above the expected suggesting possible post-translation modifications.

A number of transcription factors were also identified in the re-growing nerve, such as: the LacI family transcription regulator (proteolysis substrates/down-regulated), also identified in WH events, but with a M above the expected; the regulatory protein Crp (identified in 4 different 2DE spots both as proteolysis substrates/down-regulated and as a fragment); the transcription factor Sox-12 (fragment), already described as being elevated in the DRG cell body after injury [85] and also known to be involved in the Wnt signaling pathway, which also regulates axon path finding, axon remodeling, dendrite morphogenesis and synapse formation [86]; and the transcriptional activator Rgg/GadR/MutR (proteolysis substrates).

4.3.4. *Lipid signaling*

The turnover of phosphoinositides is also implicated in neurite formation and extension [87]. Generation of phosphatidylinositol 4,5-bisphosphate (PI(4,5)P2)3 as well as phosphatidylinositol 3,4,5-trisphosphate seems to regulate neurite retraction in a growth factor-dependent manner, and several Rho family proteins are involved in the phosphoinositide signaling network in response to stimuli [88]. Phospholipase C (PLC) is a key enzyme in phosphoinositide metabolism and is involved in the generation of two second-messengers, namely diacylglycerol (DAG) and inositol 1,4,5-trisphosphate (IP3). Recently it was further shown that an isoform of PLC is an essential regulator of neuritogenesis, by suppression of the Rho signaling pathway via the down-regulation of RhoA level [64]. Both phosphoinositide dependent kinase-1 and inositol phosphosphingolipids phospholipase C (proteolysis substrate/down-regulated) were found in WH RNC suggesting that proteolytic events might be a part of the described pathway regulation.

The phosphoinositide dependent kinase-1 is also involved in upstream activation of cap-dependent protein translation, by regulating the activity of ribosomal S6 kinase and eukaryotic initiation factor 4E binding protein (reviewed in [89]). A similar initiation factor, the eukaryotic translation initiation factor 5A-1, was found to be up-regulated in WH RNC events.

Several fragments from a START domain-containing protein, a protein similar to a phosphatidylcholine transfer protein, were also identified in both regeneration stages of *M. glacialis* RNC (WH and RG). This START protein is known to be ubiquitously distributed during neuronal development of the starfish larvae *Asterina pectinifera* [90]. Although its function seems to be related with phosphatidylcholine transfer, its relation with regeneration remains unknown, being possibly related with the supply of lipids for the new axoplasmic membranes. Clearly it is regulated through proteolysis, and most probably via UPS, since it was identified in both WH and RG RNC with an apparent M above the expected and as proteolysis substrate/down-regulated.

4.3.5. *Neuroprotective proteins*

During the regeneration events, it is critical that molecules with protective functions are present, which was shown to be the case in regenerating RNC. Several antioxidant proteins were up-regulated in the WH and RG events namely, ferritin, a protein that has been described as an important molecule to control the levels of oxygen reactive species in astrocytes [91]; and peroxiredoxin like proteins, which were previously reported to be oxidized in the mouse model of axonal degeneration, indicating that axonal integrity is related to the control of oxidative stress [92].

Several proteins responsible for controlling the cellular oxidation state, managing of reactive oxygen species among other functions, were identified only in RG events, such as dihydropteridine reductase and lysozyme C, both being up-regulated. The up-regulation of lysozyme has been previously reported in distal stumps of post-injured sciatic nerve [93]. Other proteins with similar functions were found also to be modulated by proteolytic events such as, cytochrome P450 19A1; glutathione peroxidase; glutathione S-transferase 3; oxidoreductase, short chain dehydrogenase/reductase family and peroxidase among others.

5. Concluding remarks

Neuronal regeneration results from a balance between protein *de novo* synthesis and protein catabolic pathways, however the last has received considerable less attention [22].

The use of *in vitro* neuronal models already allowed an exceptional understanding of the proteolytic pathways within neuronal regeneration events; however, this knowledge is deprived of the complexity of a natural biological system. To understand the vast number of protein substrates and the proteolytic impacts on whole neuronal tissue proteomes during regenerative events, these issues need to be addressed *in vivo*. The use of *in vivo* model systems has already been recognized as the way to further elucidate the effects of this post-translational regulatory mechanism, which will be determinant to decipher the signaling pathways regulated through proteolytic events [32]. However, such large scale studies are not yet available, specially using the non-bias set of proteomic/mass spectrometry experimental approaches. These last have already been recognized as powerful tools to study proteolytic events on whole tissues [94], as demonstrated by the recently published degradome of blood and plasma coagulation reactions [95].

In the current study we examine the differential proteomes of two different stages of echinoderm RNC regeneration: wound healing (48 h–13 days PAA) and tissue re-growth (10 weeks PAA), aiming to understand which are the activated molecular pathways in each stage and how they are modulated.

Several proteins with previously described functions in nerve regeneration were identified in this proteomic study. However, the majority of them seem to be modulated through proteolytic events. For this reason, a greater emphasis is given to the proteolytic pathways, since clearly they play a major role in modulating and controlling starfish RNC proteomes during regeneration events. Furthermore, the observed abundance of protein fragments may be an indication of their role as necessary signaling molecules, which will modulate the regenerative pathways leading to the starfish successful nervous system regeneration. Additional studies to unambiguously determine protein neo N-terminal of the generated fragments are still sought. These studies will be of extreme importance to pinpoint the newly generated peptides derived from proteolysis and to understand their respective functions during neuronal regeneration.

Altogether, the results here presented, highlight echinoderms as important neuroregeneration models, which should be further explored since 1) several of the identified proteins have a recognized role in regeneration in other model organisms, thus reinforcing its potential to aid our understanding of the phenomenon; 2) many of the regeneration-related identified proteins constitute new assignments that should be further validated and tested for potential applications in vertebrate regeneration and 3) new insights into proteolytic-driven regulation of neuronal regeneration are given, emphasizing the importance of investing in metadegradomics studies, including the characterization of neo N-terminal generated fragments. Such approaches will be of extreme importance to pinpoint the newly generated peptides derived from proteolysis and to understand their respective functions during neuronal regeneration.

Supplementary data to this article can be found online at http://dx.doi.org/10.1016/j.jprot.2013.12.012.

Conflict of interest

All authors declare no financial/commercial conflicts of interest.

Acknowledgments

This work was supported by Fundação para a Ciência e Tecnologia through grant # PEst-OE/EQB/LA0004/2011; a Post-doctoral grant to Catarina Franco (SFRH/BPD/79271/2011), a research contract by the Ciência 2008 program to Romana Santos, a project grant (PTDC/MAR/104058/2008) and through the National Re-equipment Program for "Rede Nacional de Espectrometria de Massa — RNEM" (REDE/1504/RNEM/2005). We also like to acknowledge the co-financing of MALDI-TOF/TOF MS equipment by Instituto de Biologia Experimental e Tecnológica (IBET) and Instituto Gulbenkian de Ciência (IGC).

REFERENCES

[1] Schwab ME. Nogo and axon regeneration. Curr Opin Neurobiol 2004;14:118–24.
[2] Silver J, Miller JH. Regeneration beyond the glial scar. Nat Rev Neurosci 2004;5:146–56.
[3] Tang BL. Inhibitors of neuronal regeneration: mediators and signaling mechanisms. Neurochem Int 2003;42:189–203.
[4] Sodergren E, Weinstock G, Davidson E, Cameron R, Gibbs R, Angerer R, et al. The genome of the sea urchin *Strongylocentrotus purpuratus*. Science 2006;314:941–52.
[5] Franco CF, Soares R, Pires E, Santos R, Coelho AV. Radial nerve cord protein phosphorylation dynamics during starfish arm tip wound healing events. Electrophoresis 2012;33:3764–78.
[6] García-Arrarás JE, Dolmatov IY. Echinoderms: potential model systems for studies on muscle regeneration. Curr Pharm Des 2010;16:942–55.
[7] Pasten C, Rosa R, Ortiz S, González S, García-Arrarás JE. Characterization of proteolytic activities during intestinal regeneration of the sea cucumber, *Holothuria glaberrima*. Int J Dev Biol 2012;56:681–91.
[8] Pasten C, Ortiz-Pineda PA, García-Arrarás JE. Ubiquitin–proteasome system components are upregulated during intestinal regeneration. Genesis 2012;50:350–65.
[9] Patruno M, Thorndyke MC, Candia Carnevali MD, Bonasoro F, Beesley PW. Growth factors, heat-shock proteins and regeneration in echinoderms. J Exp Biol 2001;204:843–8.
[10] Suárez-Castillo EC, Medina-Ortíz WE, Roig-López JL, García-Arrarás JE. Ependymin, a gene involved in regeneration and neuroplasticity in vertebrates, is overexpressed during regeneration in the echinoderm *Holothuria glaberrima*. Gene 2004;334:133–43.
[11] Thorndyke MC, Chen WC, Beesley PW, Patruno M. Molecular approach to echinoderm regeneration. Microsc Res Tech 2001;55:474–85.
[12] Thorndyke MC, Chen WC, Moss C, Candia Carnevali MD, Bonasoro F. Regeneration in echinoderms: cellular and molecular aspects. In: Candia Carnevali MD, Bonasoro F, editors. Echinoderm research. Balkema: Rotterdam; 1999. p. 159–64.
[13] Dupont S, Thorndyke M. Bridging the regeneration gap: insights from echinoderm models. Nat Rev Genet 2007;8:8–10.
[14] Moss C. Patterns of bromodeoxyuridine incorporation and neuropeptide immunoreactivity during arm regeneration in the starfish *Asterias rubens*. Philos Trans R Soc Lond B Biol Sci 1998;353:421–36.
[15] Huet M. Le role du sytème nerveux au cours de la régénération du Brás chez une Etoile de mer: Asterina gibbosa Penn. (Echinoderme, Astéride). J Embryol Exp Morphol 1975;33(3):535–52.
[16] Candia Carnevali MD, Burighel P. Regeneration in echinoderms and ascidians. eLS; 2010.
[17] Mashanov VS, Zueva OR, Heinzeller T. Regeneration of the radial nerve cord in a holothurian: a promising new model system for studying post-traumatic recovery in the adult nervous system. Tissue Cell 2008;40:351–72.
[18] San Miguel-Ruiz JE, Maldonado-Soto AR, García-Arrarás JE. Regeneration of the radial nerve cord in the sea cucumber *Holothuria glaberrima*. BMC Dev Biol 2009;9:3.
[19] Willis D, Li KW, Zheng J-Q, Chang JH, Smit A, Kelly T, et al. Differential transport and local translation of cytoskeletal, injury-response, and neurodegeneration protein mRNAs in axons. J Neurosci 2005;25:778–91.
[20] Yoo S, Van Niekerk EA, Merianda TT, Twiss JL. Dynamics of axonal mRNA transport and implications for peripheral nerve regeneration. Exp Neurol 2010;223:19–27.
[21] Donnelly CJ, Fainzilber M, Twiss JL. Subcellular communication through RNA transport and localized protein synthesis. Traffic 2010;11:1498–505.
[22] Gumy LF, Tan CL, Fawcett JW. The role of local protein synthesis and degradation in axon regeneration. Exp Neurol 2010;223:28–37.

[23] Spira ME, Oren R, Dormann A, Ilouz N, Lev S. Calcium, protease activation, and cytoskeleton remodeling underlie growth cone formation and neuronal regeneration. Cell Mol Neurobiol 2001;21:591–604.
[24] Sun F, Cavalli V. Neuroproteomics approaches to decipher neuronal regeneration and degeneration. Mol Cell Proteomics 2010;9:963–75.
[25] Liu RY, Snider WD. Different signaling pathways mediate regenerative versus developmental sensory axon growth. J Neurosci 2001;21:RC164.
[26] Franco M, Seyfried NT, Brand AH, Peng J, Mayor U. A novel strategy to isolate ubiquitin conjugates reveals wide role for ubiquitination during neural development. Mol Cell Proteomics 2011;10 [M110.002188].
[27] Van Niekerk EA, Willis DE, Chang JH, Reumann K, Heise T, Twiss JL. Sumoylation in axons triggers retrograde transport of the RNA-binding protein La. Proc Natl Acad Sci U S A 2007;104:12913–8.
[28] Martin S, Wilkinson KA, Nishimune A, Henley JM. Emerging extranuclear roles of protein SUMOylation in neuronal function and dysfunction. Nat Rev Neurosci 2007;8:948–59.
[29] Van Domselaar R, De Poot SAH, Bovenschen N. Proteomic profiling of proteases: tools for granzyme degradomics. Expert Rev Proteomics 2010;7:347–59.
[30] Saxena S, Singh SK, Meena Lakshmi MG, Meghah V, et al. Proteomic analysis of zebrafish caudal fin regeneration. Mol Cell Proteomics 2012:1–51.
[31] Pizzi MA, Crowe MJ. Matrix metalloproteinases and proteoglycans in axonal regeneration. Exp Neurol 2007;204:496–511.
[32] Page-McCaw A. Remodeling the model organism: matrix metalloproteinase functions in invertebrates. Semin Cell Dev Biol 2008;19:14–23.
[33] Quiñones JL, Rosa R, Ruiz DL, García-Arrarás JE. Extracellular matrix remodeling and metalloproteinase involvement during intestine regeneration in the sea cucumber Holothuria glaberrima. Dev Biol 2002;250:181–97.
[34] Gitler D, Spira ME. Real time imaging of calcium-induced localized proteolytic activity after axotomy and its relation to growth cone formation. Neuron 1998;20:1123–35.
[35] Perlson E, Medzihradszky KF, Darula Z, Munno DW, Syed NI, Burlingame AL, et al. Differential proteomics reveals multiple components in retrogradely transported axoplasm after nerve injury. Mol Cell Proteomics 2004;3:510–20.
[36] Perlson E, Hanz S, Ben-Yaakov K, Segal-Ruder Y, Seger R, Fainzilber M. Vimentin-dependent spatial translocation of an activated MAP kinase in injured nerve. Neuron 2005;45:715–26.
[37] Perlson E, Michaelevski I, Kowalsman N, Ben-Yaakov K, Shaked M, Seger R, et al. Vimentin binding to phosphorylated Erk sterically hinders enzymatic dephosphorylation of the kinase. J Mol Biol 2006;364:938–44.
[38] Glickman MH, Ciechanover A. The ubiquitin–proteasome proteolytic pathway: destruction for the sake of construction. Physiol Rev 2002;82:373–428.
[39] Kaang B-K, Choi J-H. Synaptic protein degradation in memory reorganization. Adv Exp Med Biol 2012;970:221–40.
[40] Hegde AN, Upadhya SC. Role of ubiquitin–proteasome-mediated proteolysis in nervous system disease. Biochim Biophys Acta 1809;2011:128–40.
[41] Upadhya SC, Hegde AN. Role of the ubiquitin proteasome system in Alzheimer's disease. BMC Biochem 2007;8(Suppl. 1):S12.
[42] Klimaschewski L. Ubiquitination and proteasomal protein degradation in neurons. In: Lajtha A, Banik N, editors. Handbook of neurochemistry and molecular neurobiology. Boston, MA: Springer US; 2007. p. 653–62.
[43] Verma P, Chierzi S, Codd AM, Campbell DS, Meyer RL, Holt CE, et al. Axonal protein synthesis and degradation are necessary for efficient growth cone regeneration. J Neurosci 2005;25:331–42.
[44] Savedia S, Kiernan JA. Increased production of ubiquitin mRNA in motor neurons after axotomy. Neuropathol Appl Neurobiol 1994;20:577–86.
[45] Butt RH, Coorssen JR. Pre-extraction sample handling by automated frozen disruption significantly improves subsequent proteomic analyses. J Proteome Res 2006;5:437–48.
[46] Neuhoff V, Arold N, Taube D, Ehrhardt W. Improved staining of 500 proteins in polyacrylamide gels including isoelectric focusing 501 gels with clear background at nanogram sensitivity using 502 coomassie brilliant blue G-250 and R-250. Electrophoresis 1988;9:255–62.
[47] Franco CF, Santos R, Coelho AV. Exploring the proteome of an echinoderm nervous system: 2-DE of the sea star radial nerve cord and the synaptosomal membranes subproteome. Proteomics 2011;11:1359–64.
[48] Lietzén N, Natri L, Nevalainen OS, Salmi J, Nyman TA. Compid: a new software tool to integrate and compare MS/MS based protein identification results from Mascot and Paragon. J Proteome Res 2010;9:6795–800.
[49] Franco CF, Santos R, Coelho AV. Proteome characterization of sea star coelomocytes — the innate immune effector cells of echinoderms. Proteomics 2011;11:3587–92.
[50] Moss C. Philos Trans R Soc Lond B Biol Sci 1998;353:421–36.
[51] Hernroth B, Farahani F, Brunborg G, Dupont S, Dejmek A, Sköld HN. Possibility of mixed progenitor cells in sea star arm regeneration. J Exp Zool B Mol Dev Evol 2010;314:457–68.
[52] Mladenov PV, Bisgrove B, Asotra S, Burke RD. Roux's Arch Dev Biol 1989;198:19–28.
[53] Fan T, Fan X, Du Y, Sun W, et al. J Ocean Univ Chin 2011;10: 255–62.
[54] Thorndyke MC, Chen WC, Beesley PW, Patruno M. Microsc Res Tech 2001;55:474–85.
[55] Jiménez CR, Stam FJ, Li KW, Gouwenberg Y, Hornshaw MP, De Winter F, et al. Proteomics of the injured rat sciatic nerve reveals protein expression dynamics during regeneration. Mol Cell Proteomics 2005;4:120–32.
[56] Tai H-C, Schuman EM. Ubiquitin, the proteasome and protein degradation in neuronal function and dysfunction. Nat Rev Neurosci 2008;9:826–38.
[57] Ambron RT, Walters ET. Priming events and retrograde injury signals. A new perspective on the cellular and molecular biology of nerve regeneration. Mol Neurobiol 1996;13:61–79.
[58] Lowery LA, Van Vactor D. The trip of the tip: understanding the growth cone machinery. Nat Rev Mol Cell Biol 2009;10:332–43.
[59] Stiess M, Bradke F. Neuronal polarization: the cytoskeleton leads the way. Dev Neurobiol 2011;71:430–44.
[60] Hall A, Lalli G. Rho and Ras GTPases in axon growth, guidance, and branching. Cold Spring Harb Perspect Biol 2010;2:a001818.
[61] Takenawa T, Miki H. WASP and WAVE family proteins: key molecules for rapid rearrangement of cortical actin filaments and cell movement. J Cell Sci 2001;114:1801–9.
[62] Nobes CD, Hall A. Rho, rac, and cdc42 GTPases regulate the assembly of multimolecular focal complexes associated with actin stress fibers, lamellipodia, and filopodia. Cell 1995;81:53–62.
[63] Garvalov BK, Flynn KC, Neukirchen D, Meyn L, Teusch N, Wu X, et al. Cdc42 regulates cofilin during the establishment of neuronal polarity. J Neurosci 2007;27:13117–29.
[64] Kouchi Z, Igarashi T, Shibayama N, Inanobe S, Sakurai K, Yamaguchi H, et al. Phospholipase Cdelta3 regulates RhoA/Rho kinase signaling and neurite outgrowth. J Biol Chem 2011;286:8459–71.
[65] Wang H-R, Zhang Y, Ozdamar B, Ogunjimi AA, Alexandrova E, Thomsen GH, et al. Regulation of cell polarity and

protrusion formation by targeting RhoA for degradation. Science 2003;302:1775–9.
[66] Kim YS, Furman S, Sink H, VanBerkum MF. Calmodulin and profilin coregulate axon outgrowth in Drosophila. J Neurobiol 2001;47:26–38.
[67] McCallum SJ, Wu WJ, Cerione RA. Identification of a putative effector for Cdc42Hs with high sequence similarity to the RasGAP-related protein IQGAP1 and a Cdc42Hs binding partner with similarity to IQGAP2. J Biol Chem 1996;271:21732–7.
[68] Autieri MV, Kelemen SE, Wendt KW. AIF-1 is an actin-polymerizing and Rac1-activating protein that promotes vascular smooth muscle cell migration. Circ Res 2003;92:1107–14.
[69] Bennett V, Baines AJ. Spectrin and ankyrin-based pathways: metazoan inventions for integrating cells into tissues. Physiol Rev 2001;81:1353–92.
[70] Holleran EA, Ligon LA, Tokito M, Stankewich MC, Morrow JS, Holzbaur EL. beta III spectrin binds to the Arp1 subunit of dynactin. J Biol Chem 2001;276:36598–605.
[71] Erez H, Malkinson G, Prager-Khoutorsky M, De Zeeuw CI, Hoogenraad CC, Spira ME. Formation of microtubule-based traps controls the sorting and concentration of vesicles to restricted sites of regenerating neurons after axotomy. J Cell Biol 2007;176:497–507.
[72] Lewcock JW, Genoud N, Lettieri K, Pfaff SL. The ubiquitin ligase Phr1 regulates axon outgrowth through modulation of microtubule dynamics. Neuron 2007;56:604–20.
[73] Kono K, Saeki Y, Yoshida S, Tanaka K, Pellman D. Proteasomal degradation resolves competition between cell polarization and cellular wound healing. Cell 2012;150:1–14.
[74] Reyes-Turcu FE, Ventii KH, Wilkinson KD. Regulation and cellular roles of ubiquitin-specific deubiquitinating enzymes. Annu Rev Biochem 2009;78:363–97.
[75] Glogowska A, Pyka J, Kehlen A, Los M, Perumal P, Weber E, et al. The cytoplasmic domain of proEGF negatively regulates motility and elastinolytic activity in thyroid carcinoma cells1. Neoplasia 2008;10:1120–30.
[76] Morihara T, Mizoguchi A, Takahashi M, Kozaki S, Tsujihara T, Kawano S, et al. Distribution of synaptosomal-associated protein 25 in nerve growth cones and reduction of neurite outgrowth by botulinum neurotoxin A without altering growth cone morphology in dorsal root ganglion neurons and PC-12 cells. Neuroscience 1999;91:695–706.
[77] Tessier-Lavigne M, Goodman CS. The molecular biology of axon guidance. Science 1996;274:1123–33.
[78] Brose K, Bland KS, Wang KH, Arnott D, Henzel W, Goodman CS, et al. Slit proteins bind Robo receptors and have an evolutionarily conserved role in repulsive axon guidance. Cell 1999;96:795–806.
[79] Battye R, Stevens A, Jacobs JR. Axon repulsion from the midline of the Drosophila CNS requires slit function. Development 1999;126:2475–81.
[80] Quinn CC, Gray GE, Hockfield S. A family of proteins implicated in axon guidance and outgrowth. J Neurobiol 1999;41:158–64.
[81] Oliver JD, Roderick HL, Llewellyn DH, High S. ERp57 functions as a subunit of specific complexes formed with the ER lectins calreticulin and calnexin. Mol Biol Cell 1999;10:2573–82.
[82] Jascur T, Brickner H, Salles-Passador I, Barbier V, El Khissiin A, Smith B, et al. Regulation of p21(WAF1/CIP1) stability by WISp39, a Hsp90 binding TPR protein. Mol Cell 2005;17:237–49.
[83] Abe N, Cavalli V. Nerve injury signaling. Curr Opin Neurobiol 2008;18:276–83.
[84] Chen J, Morosan-Puopolo G, Dai F, Wang J, Brand-Saberi B. Molecular cloning of chicken Cecr2 and its expression during chicken embryo development. Int J Dev Biol 2010;54:925–9.
[85] Tanabe K, Bonilla I, Winkles JA, Strittmatter SM. Fibroblast growth factor-inducible-14 is induced in axotomized neurons and promotes neurite outgrowth. J Neurosci 2003;23:9675–86.
[86] Ciani L, Salinas PC. WNTs in the vertebrate nervous system: from patterning to neuronal connectivity. Nat Rev Neurosci 2005;6:351–62.
[87] Arimura N, Kaibuchi K. Neuronal polarity: from extracellular signals to intracellular mechanisms. Nat Rev Neurosci 2007;8:194–205.
[88] Santarius M, Lee CH, Anderson RA. Supervised membrane swimming: small G-protein lifeguards regulate PIPK signalling and monitor intracellular PtdIns(4,5)P2 pools. Biochem J 2006;398:1–13.
[89] Liu K, Tedeschi A, Park KK, He Z. Neuronal intrinsic mechanisms of axon regeneration. Annu Rev Neurosci 2011;34:131–52.
[90] Murabe N, Hatoyama H, Hase S, Komatsu M, Burke RD, Kaneko H, et al. Neural architecture of the brachiolaria larva of the starfish, *Asterina pectinifera*. J Comp Neurol 2008;509:271–82.
[91] Regan RF, Kumar N, Gao F, Guo Y. Ferritin induction protects cortical astrocytes from heme-mediated oxidative injury. Neuroscience 2002;113:985–94.
[92] Mi W, Beirowski B, Gillingwater TH, Adalbert R, Wagner D, Grumme D, et al. The slow Wallerian degeneration gene, WldS, inhibits axonal spheroid pathology in gracile axonal dystrophy mice. Brain 2005;128:405–16.
[93] Kubo T, Yamashita T, Yamaguchi A, Hosokawa K, Tohyama M. Analysis of genes induced in peripheral nerve after axotomy using cDNA microarrays. J Neurochem 2002;82:1129–36.
[94] Doucet A, Butler GS, Rodríguez D, Prudova A, Overall CM. Metadegradomics: toward in vivo quantitative degradomics of proteolytic post-translational modifications of the cancer proteome. Mol Cell Proteomics 2008;7:1925–51.
[95] Niessen S, Hoover H, Gale AJ. Proteomic analysis of the coagulation reaction in plasma and whole blood using PROTOMAP. Proteomics 2011;11:2377–88.
[96] Giniger E. How do Rho family GTPases direct axon growth and guidance? A proposal relating signaling pathways to growth cone mechanics. Differ Res Biol Divers 2002;70:385–96.
[97] Kozma R, Sarner S, Ahmed S, Lim L. Rho family GTPases and neuronal growth cone remodelling: relationship between increased complexity induced by Cdc42Hs, Rac1, and acetylcholine and collapse induced by RhoA and lysophosphatidic acid. Mol Cell Biol 1997;17:1201–11.
[98] Andersen SSL. The search and prime hypothesis for growth cone turning. Bioessays 2005;27:86–90.
[99] Rajnicek AM, Foubister LE, McCaig CD. Growth cone steering by a physiological electric field requires dynamic microtubules, microfilaments and Rac-mediated filopodial asymmetry. J Cell Sci 2006;119:1736–45.